NTNU – Trondheim
Norwegian University of
Science and Technology

Conduit Dynamics in Herand Power Plant

Siri Skyberg Sletten

Master of Energy and Environmental Engineering
Submission date: June 2015
Supervisor: Pål Tore Selbo Storli, EPT
Co-supervisor: Torbjørn Nielsen, EPT

Norwegian University of Science and Technology
Department of Energy and Process Engineering

NTNU
Norges teknisk-naturvitenskapelige universitet

Institutt for energi- og prosessteknikk

EPT-M-2015-83

MASTEROPPGAVE

for

Siri Skyberg Sletten

Våren 2015

Vannveisdynamikk i Herand Kraftverk

Conduit dynamics in Herand Power plant

Bakgrunn og målsetting

Etableringen av Herand Kraftverk er i forberedende prosess for en konsesjonssøknad. Størrelsen på dette kraftverket gjør at det faller inn under Statnett sine krav til at man skal ha frekvensregulering og at man skal kunne operere på isolert nett. Reguleringsegenskapene til dette kraftverket vil derimot by på en utfordring, og tiltak som forbedrer reguleringsegenskapene vil fort bli kostbare. I prosjektoppgaven ble Herand kraftverk utstyrt med luftputekammer undersøkt. Det er ønskelig å undersøke dette alternativet videre med tanke på reguleringsstabilitet og stabilitetsegenskaper, spesielt med tanke på at dette blir et kraftverk uten særlige muligheter til å øke produksjonen ut over den mengden vann som naturlig renner ut fra Fodnastølsvatnet.
Stabilitetsanalyse utføres vanligvis ved hjelp av transferfunksjoner og resulterer i AFF-diagrammer som tolkes. Transferfunksjonene finnes ved hjelp av ligninger som er lineariserte omkring et driftspunkt og hvilket driftspunkt man velger å analysere har således en innvirkning på ligningene. Det er viktig at man undersøker reguleringsstabiliteten for kraftverket i de tilfeller der den tilgjengelige vannmengden er begrenset grunnet liten volumstrøm ut av Fodnastølsvatnet.

Mål

Studenten skal gjennomføre en detaljert stabilitetsanalyse for å undersøke stabilitetsegenskapene til Herand kraftverk med og uten luftputekammer. Forskjellige driftspunkt skal undersøkes med tanke på at kraftverket skal være stabilt og kunne operere på eget nett også når tilgjengelig vannmengde er liten samt at nødvendig størrelse på luftputekammeret må bestemmes.

Oppgaven bearbeides ut fra følgende punkter

1. Litteraturstudie på temaene vannveisdynamikk, regulering og stabilitet
2. Gjennomføre en detaljert stabilitetsanalyse på Herand kraftverk; med og uten luftputekammer for forskjellige driftspunkt
3. Bestemme den nødvendige størrelsen på luftputekammeret avhengig av resultatene fra stabilitetsanalysen

" - "

Senest 14 dager etter utlevering av oppgaven skal kandidaten levere/sende instituttet en detaljert fremdrift- og eventuelt forsøksplan for oppgaven til evaluering og eventuelt diskusjon med faglig ansvarlig/veiledere. Detaljer ved eventuell utførelse av dataprogrammer skal avtales nærmere i samråd med faglig ansvarlig.

Besvarelsen redigeres mest mulig som en forskningsrapport med et sammendrag både på norsk og engelsk, konklusjon, litteraturliste, innholdsfortegnelse etc. Ved utarbeidelsen av teksten skal kandidaten legge vekt på å gjøre teksten oversiktlig og velskrevet. Med henblikk på lesning av besvarelsen er det viktig at de nødvendige henvisninger for korresponderende steder i tekst, tabeller og figurer anføres på begge steder. Ved bedømmelsen legges det stor vekt på at resultatene er grundig bearbeidet, at de oppstilles tabellarisk og/eller grafisk på en oversiktlig måte, og at de er diskutert utførlig.

Alle benyttede kilder, også muntlige opplysninger, skal oppgis på fullstendig måte. For tidsskrifter og bøker oppgis forfatter, tittel, årgang, sidetall og eventuelt figurnummer.

Det forutsettes at kandidaten tar initiativ til og holder nødvendig kontakt med faglærer og veileder(e). Kandidaten skal rette seg etter de reglementer og retningslinjer som gjelder ved alle (andre) fagmiljøer som kandidaten har kontakt med gjennom sin utførelse av oppgaven, samt etter eventuelle pålegg fra Institutt for energi- og prosessteknikk.

Risikovurdering av kandidatens arbeid skal gjennomføres i henhold til instituttets prosedyrer. Risikovurderingen skal dokumenteres og inngå som del av besvarelsen. Hendelser relatert til kandidatens arbeid med uheldig innvirkning på helse, miljø eller sikkerhet, skal dokumenteres og inngå som en del av besvarelsen. Hvis dokumentasjonen på risikovurderingen utgjør veldig mange sider, leveres den fulle versjonen elektronisk til veileder og et utdrag inkluderes i besvarelsen.

I henhold til "Utfyllende regler til studieforskriften for teknologistudiet/sivilingeniørstudiet" ved NTNU § 20, forbeholder instituttet seg retten til å benytte alle resultater og data til undervisnings- og forskningsformål, samt til fremtidige publikasjoner.

Besvarelsen leveres digitalt i DAIM. Et faglig sammendrag med oppgavens tittel, kandidatens navn, veileders navn, årstall, instituttnavn, og NTNUs logo og navn, leveres til instituttet som en separat pdf-fil. Etter avtale leveres besvarelse og evt. annet materiale til veileder i digitalt format.

☐ Arbeid i laboratorium (vannkraftlaboratoriet, strømningsteknisk, varmeteknisk)
☐ Feltarbeid

NTNU, Institutt for energi- og prosessteknikk, 14. januar 2015

Olav Bolland
Instituttleder

Pål-Tore Storli
Faglig ansvarlig/veileder

Torbjørn Nielsen, Vannkraftlaboratoriet EPT NTNU
Ingunn Granstrøm, Skagerak Kraft

Abstract

The aim of this master thesis was to conduct a stability analysis of Herand power plant. Herand is a hydropower plant under planning by Herand Kraft, and it is planned to have a generator of 27MVA. The size of the power plant puts it under the requirements in Norway stating that all generators above 10MVA must have frequency regulation and be able to operate in an isolated grid. This paper presents a conducted analysis of Herand that examines whether the plant will be able to meet these requirements, and maintain a stable regulation system.

The conducted analysis was based on control theory. A block diagram was set up from differential equations for each element in Herand power plant. The transfer function of the system was found, and by the use of Simulink and Matlab, as well as an analytical approach, the Amplitude - Phase - Frequency (APF) diagrams were found. The focus in the analysis was three dynamic aspects; the mass oscillations between inlet and air cushion surge chamber, water hammer occuring in the penstock following a regulation when including the elastic property of the penstock, and regulation stability.

The challenge for Herand when it comes to obtaining acceptable frequency regulation is concerning the topography at the location. The penstock will be long, and an air cushion surge chamber will be implemented upstream of the turbine to enhance stability. An objective of this paper was to find the optimal dimensions of the air cushion surge chamber, and to examine whether Herand then will have acceptable regulation stability.

The conducted simulations showed that Herand power plant will have a stable regulation system when implementing an air cushion surge chamber. The elastic frequency will lie above the crossover frequency, hence the controller will not attempt to regulate the pressure surges. The system will be unstable without an air cushion surge chamber. The Thoma critical area was calculated to find the minimum required surface area of the air cushion that will result in stable mass oscillations. The total volume of the air cushion surge chamber used in the simulations was $712.26m^3$. Up- and downsurge from the air cushion surge chamber was also avoided with the calculated volume.

Sammendrag

Målet med denne masteroppgaven var å gjennomføre en stabilitetsanalyse av Herand kraftverk. Herand er et vannkraftverk under planlegging av Herand Kraft, og det skal ha en generator på 27MVA. Størrelsen på kraftverket gjør at det faller inn under Statnetts krav om at alle kraftverk med generator på 10MVA eller mer må ha frekvensregulering og må kunne operere på isolert nett. I denne oppgaven ble det gjennomført en analyse av Herand for å undersøke om kraftverket vil være i stand til å møte disse kravene, og å opprettholde et stabilt reguleringssystem.

Den gjennomførte analysen er basert på reguleringsteknikk. Et blokkdiagram ble satt opp basert på differensialligningene til hvert element i Herand. Transferfunksjonen til systemet ble funnet, og ved bruk av Matlab og Simulink, samt en analytisk metode, ble Amplitude – Fase – Frekvens-diagrammene generert. Fokuset i analysen var på tre dynamiske aspekter; massesvingninger mellom inngang og luftputekammer, vannhammereffekt i røret etter en regulering når man inkluderer elastiske effekter, og reguleringsstabilitet.

Utfordringen for Herand kraftverk med hensyn på å oppnå akseptable reguleringsegenskaper er topografien på stedet. Røret vil være langt, og et luftputekammer skal plasseres oppstrøms turbinen for å forbedre stabiliteten. Et mål med denne oppgaven var å finne optimale dimensjoner på luftputekammeret, samt å undersøke om Herand da vil oppnå akseptabel reguleringsstabilitet.

De gjennomførte simuleringene viste at Herand kraftverk vil oppnå et stabilt reguleringssystem når et luftputekammer er inkludert. Den elastiske frekvensen vil ligge over kryssfrekvensen, og dermed vil regulatoren ikke prøve å regulere trykkstøtene. Systemet vil være ustabilt uten luftputekammer. Thoma-tverrsnittet ble kalkulert for å finne minimum overflateareal på luftputen som vil gi stabile massesvingninger. Det totale volumet på luftputekammeret var $712.26m^3$. Opp- og nedsving fra luftputekammeret vil også unngås med det beregnede volumet.

Preface

This master thesis has been written at the Waterpower Laboratory at the Norwegian University of Science and Technology at the Department of Energy and Process Engineering during the spring of 2015.

First and foremost I would like to thank my supervisor, Pål-Tore Selbo Storli, for great guidance and help whenever I needed it. I would also like to thank my co-supervisor, Torbjørn K. Nielsen, for all his help.

Siri Skyberg Sletten
Trondheim, spring 2015

Contents

List of Figures

List of Tables

1 Introduction

99 percent of all power generation in Norway comes from hydropower, and globally, hydropower stands for about 1/6 of power production [5]. It is a renewable and reliable energy source, and can be regulated faster than other renewable energy sources. Its ability to regulate production fast makes it a favorable energy source when it comes to maintaining a stable frequency in the electrical grid.

A balance between consumption and production in the electrical grid has to be maintained at all times. If for example, a light is switched on and consumption increases, a power plant has to increase production by the same amount. This is to maintain a continuous balance in the power system and grid frequency. Due to deviations in required power output of the grid, there will constantly occur small imbalances in grid frequency that need to be corrected for. It is highly important to maintain a stable grid frequency to avoid damage on electrical equipment. In Norway the nominal grid frequency is 50Hz. Acceptable steady-state deviation is ± 0.1Hz [6]. The Norwegian grid is connected to the Nordic electricity grid, and hence it is affected by frequency deviation in the electrical grid in the other Nordic countries.

Hydropower is the only renewable energy source with the ability to regulate production fast. For example is wind power generation dependent on the available wind at a certain location at a certain time. This applies to solar power generation as well, because these energy sources cannot be stored for utilization at a later time. With hydropower however, water can be stored in a reservoir connected to the hydropower plant when there is excess of natural inflow. This water can be utilized later when consumption increases or at times of low natural inflow. Due to this, hydropower plants have the role of frequency regulators.

The Norwegian hydropower plants take a lot of the frequency regulation in the Nordic grid and must be able to increase or decrease production quickly to maintain the balance in the grid. Therefore there is a requirement in Norway that all power plants with an installed capacity above 10MVA must have frequency regulation and be able

to operate in an isolated grid [7].

1.1 Background

This paper will investigate the hydropower plant Herand. Simulations of Herand power plant will be conducted using the computer programs Simulink and Matlab as well as an analytical approach, and the stability of Herand's regulation system will be examined by the use of APF diagrams. Based on the simulations conducted, the optimal dimensions of the air cushion surge chamber upstream the turbine will be found, and whether Herand will obtain an acceptable regulation stability will be examined.

2 Theory

Sometimes a mathematical model is needed to describe a physical system, such as a hydropower plant, so that the physical system can be modelled. In the following section, the differential equations for the different elements of a hydropower plant will be presented. The elements that will be presented are the following:

Penstock
Surge shaft
Turbine/Generator
Controller

The differential equations describe the behavior of the system. The differential equations were linearized around an operating point, and then Laplace transformed and set up in a block diagram. Further on, the transfer function of the system was found, which was used to obtain an Amplitude - Phase - Frequency (APF) diagram. APF diagrams are used when conducting a stability analysis of a hydropower plant.

2.1 Time Constants

To obtain stable operation of a hydropower system, it is important to dimension the plant correctly. The main parameters stability depends on are the time constant for the inertia of the water masses T_w, and the time constant for the rotating masses T_a. The ratio T_a/T_w should be > 6 to obtain acceptable regulation stability in a system [8]. However, if the penstock is long and the elasticity effects of the penstock and the compressibility of water are included, the criteria T_a/T_w is not sufficient. It is therefore important to include the elastic property of the penstock. This will be further discussed later in this chapter.

2.2 Penstock

The differential equations for a water column are forms of the continuity equation and the equation of motion. The continuity equation states that the accumulated volume for an area of a water column equals the volumetric flow in to the area minus the volumetric flow out. Rearranging and fixing give the following form of the continuity equation for a water column [9]:

$$\frac{\partial H}{\partial t} + \frac{a^2}{g}\frac{\partial v}{\partial x} = 0 \tag{2.1}$$

The equation of motion for a water column is derived from Newton's 2nd law applied to a water column, rearranged and fixed. For full derivation, see Torbjørn Nielsen's compendium [9]. The equation of motion for a water column becomes:

$$g\frac{\partial H}{\partial x} + \frac{\partial v}{\partial t} + f\frac{v\,|v|}{2D} = 0 \tag{2.2}$$

Where $H = h + z$ = hydraulic pressure + height
$a = \sqrt{\frac{K}{\rho}}$, is the speed of sound in water
g is the gravitational acceleration
$v = \frac{Q}{A}$ is the velocity
f is the friction factor
D is the pipe diameter

The last term of the equation of motion accounts for the loss in the penstock. The hydraulic losses along the pipe in stationary flow is on the form:

$$\Delta h = kQ^2 \tag{2.3}$$

This model assumes a fully developed, turbulent velocity profile, and will hold in cases of turbulent flow conditions around the operating point. For stationary flow conditions however, the damping effects from frictional forces will be underestimated [9].

2.3 Shaft

For the branching between shaft and pipe, the continuity equation states that the volumetric flow in the tunnel prior to the shaft is equal to the volumetric flow going

up in the shaft plus the volumetric flow in the tunnel after the shaft (Equation 2.4) [9].

$$Q_{in} = Q_{out} + Q_{up} \tag{2.4}$$

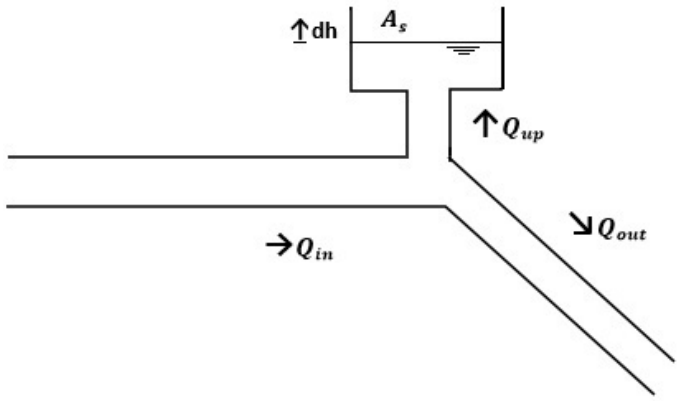

Figure 2.1: Surge shaft

Q_{up} is the volumetric flow flowing up in the shaft. It can be represented by the shaft area and the change in water level in the shaft, as illustrated in the equation below.

$$Q_{up} = A_s \frac{dh}{dt} \tag{2.5}$$

Inserting this into Equation 2.4 gives the differential equation for the shaft oscillations.

$$Q_{in} = Q_{out} + A_s \frac{dh}{dt} \tag{2.6}$$

$$\frac{dh}{dt} = \frac{1}{A_s}(Q_{in} - Q_{out}) \tag{2.7}$$

2.4 Turbine

The hydraulic head of a hydropower plant is utilized to gain kinetic energy, which in turn is transformed to mechanical energy in the turbine. The hydraulic power rotates the turbine, which is attached to the generator by a shaft, thus generating

electrical energy. The hydraulic power P_h goes to acceleration of the rotating masses, electrical efficiency to the grid P_N and loss [9].

$$P_h = J\omega\frac{d\omega}{dt} + P_N + loss \tag{2.8}$$

Or

$$J\omega\frac{d\omega}{dt} = P_h - P_N - loss \tag{2.9}$$

Where $P_h = \rho gQH$
P_N is the electrical efficiency to the grid
M is the momentum $= J\frac{d\omega}{dt}$
ω is the polar moment of inertia

2.5 Controller

The controller regulates the guide vane position, and thus volumetric flow through the turbine, based on required output and input. The PID controller have three constant parameters, which are the proportional(P), the integral(I) and the derivative(D). The equation for the PID controller is [9]:

$$\Delta y = -k_p\Delta n - \frac{k_p}{T_d}\int \Delta n dt - k_p T_n \Delta n \tag{2.10}$$

Where y = opening degree
k_p is the gain
n is the rotational speed
T_d is the integral term
T_n is the derivative term

The terms in Equation 2.10 are respectively the P, I and D terms. The proportional term uses the error between setpoint value and the measurable value, which is multiplied by a constant. The integral term depends on past errors. The derivative term is based on the slope of the error.

2.6 Dynamic Equations

The equations used for each element of the hydropower system are previously presented. The following section presents how to simplify the model and combine the differential equations to a complete block diagram in the frequency domain.

The method described in the following section is to linearize the differential equations, Laplace transform, and obtain equations using the relations $h = \frac{\Delta H}{H_0}$, $q = \frac{\Delta Q}{Q_0}$, $\nu = \frac{\Delta P}{P_0}$ and $\mu = \frac{\Delta n}{n_0}$. The complete derivations are found in Appendix A, and a shortened version is shown below.

2.6.1 Waterway

The equation of motion is presented above. By rearranging and fixing (shown in Appendix A), the equation becomes:

$$\frac{L}{gA}\frac{dQ}{dt} + \Delta H + KQ|Q| = 0 \tag{2.11}$$

Where $K = f\frac{L}{2gA^2D}$

No losses in the waterway was assumed here for simplicity. Linearizing and Laplace transforming Equation 2.11 give:

$$h = -T_w s q \tag{2.12}$$

The equation for turbine opening degree is per definition:

$$\kappa = \frac{\frac{Q}{\sqrt{2gH}}}{\frac{Q_{design}}{\sqrt{2gH_{design}}}} \tag{2.13}$$

Or

$$\kappa = \frac{Q}{Q_{design}}\frac{\sqrt{2gH_{design}}}{\sqrt{2gH}} \tag{2.14}$$

Derivation of the equation above, and then linearizing give:

$$q = \frac{1}{2}h \tag{2.15}$$

Using the same method for the equation for power absorbed in the turbine $P_h = \eta\rho g Q H$ gives:

$$P_h = q + h \tag{2.16}$$

Combining the equations for the waterway gives the block diagram illustrated in Figure 2.2, where $T_w = \frac{Q_0}{gH_0}\frac{L}{A}$.

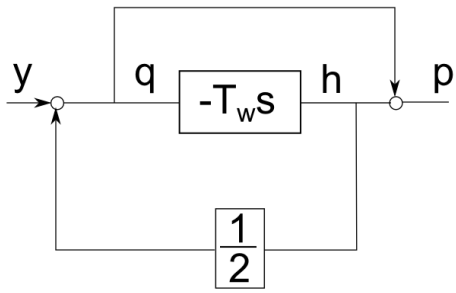

Figure 2.2: Block diagram of waterway

The transfer function for the waterway, and reduction of the block diagram is [9]:

$$\frac{p}{y} = \frac{1 - T_w s}{1 + 0.5 T_w s} \tag{2.17}$$

2.6.2 Surge Shaft

The equation for changes in water level in the shaft is:

$$\frac{dh}{dt} = \frac{1}{A_s}(Q_{in} - Q_{out}) \tag{2.18}$$

Linearizing and Laplace transforming give:

$$shH_0 = \frac{1}{A_s}(q_{in} - q_{out})Q_0 \tag{2.19}$$

The final form of the shaft equation thus becomes:

$$h = \frac{1}{T_{up}}q_{up} \tag{2.20}$$

Where $T_{up} = \frac{A_s H_0}{Q_0}$.

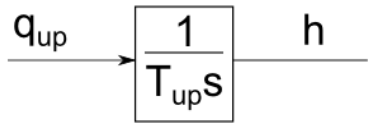

Figure 2.3: Block diagram of surge shaft

2.6.3 Turbine Inertia

As previously presented, the equation for the turbine inertia is:

$$J\omega\frac{d\omega}{dt} = P_h - P_N = \Delta P \tag{2.21}$$

Linearizing, Laplace transforming and using the relations give the following relation.

$$\mu = \frac{1}{T_a s}\nu \tag{2.22}$$

The block diagram for the turbine inertia is illustrated in Figure 2.4.

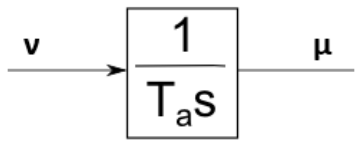

Figure 2.4: Block diagram of turbine inertia

2.6.4 Controller

The differential equation equation for a PID controller is the following [9].

$$\frac{dy}{dt} = -k_p \frac{dn}{dt} + \frac{k_p}{T_d}(n_0 - n) - k_p T_n \frac{d^2 n}{dt^2} \tag{2.23}$$

Laplace transforming and rearranging give:

$$\frac{y}{\mu} = \frac{1}{b_t}(1 - \frac{1}{T_d s} + T_n s) \tag{2.24}$$

The block diagram for the PID controller is illustrated in Figure 2.5.

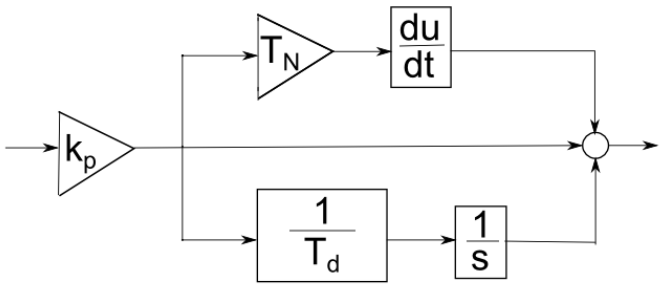

Figure 2.5: Block diagram of PID controller

2.7 Combined Block Diagram

The complete system was found by combining the block diagrams of the subsystems described above. The block diagram in Figure 2.6 does not include a surge shaft, for simplicity. The complete block diagram including surge shaft will be presented later in this paper.

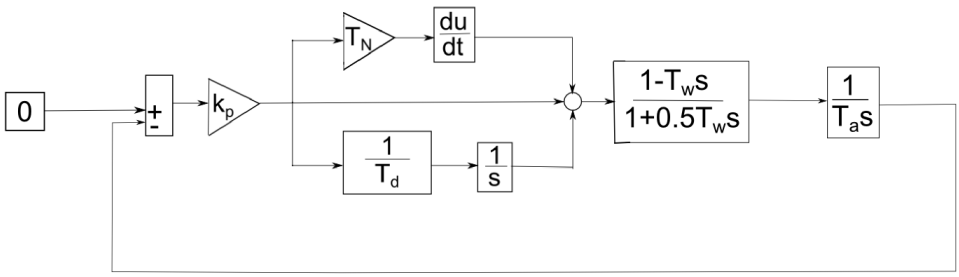

Figure 2.6: Combined block diagram excluding surge shaft

2.8 Including elasticity effects

In this paper, there are two approaches to modelling the penstock in a hydropower system. Rigid theory assumes a rigid pipe and water column, and this approach was presented in the section above. The other approach includes the elasticity of the penstock and the compressibility of the water column. A hydropower system with a long penstock must include the elastic property of the penstock, while a short penstock can be assumed inelastic [8]. The difference between the rigid theory-based block diagram in the section above and one where the elasticity effects are included, is a hyperbolic tangent term. The term is unstable, and behaves as the tan-function, because as x approaches $\pm\frac{\pi}{2}$, it approaches $\pm\infty$ [8]. The block diagrams for the controller and the turbine inertia remain the same, while the block diagram for the waterway becomes as illustrated in Figure 2.7, when including elasticity effects.

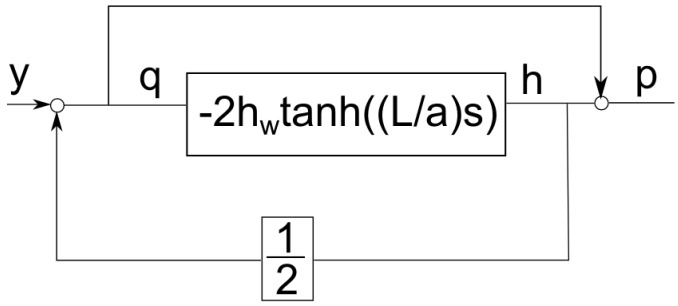

Figure 2.7: Block diagram for waterway including elastic property

The transfer function, and reduction of the waterway, for the elastic waterway in Figure 2.7 is [8]:

$$\frac{p}{y} = \frac{1 - 2h_w \tanh(\frac{L}{a}s)}{1 + h_w \tanh(\frac{L}{a}s)} \tag{2.25}$$

Where $s = j\omega$

2.9 Transfer Functions

The transfer function of a system can be obtained from the system's block diagram. A transfer function describes the correlation between one inlet and one outlet signal. To obtain the transfer function for a system from a block diagram, there are some useful rules to reduce the initial block diagram, which are presented in Table 2.1.

Manipulation	Original diagram	Result
Combining blocks in series	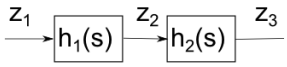	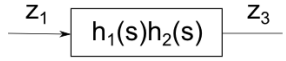
Combining blocks in parallel	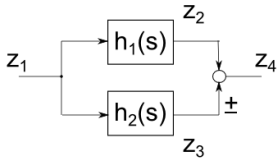	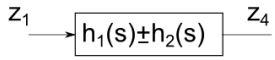
Moving a summation point behind a block	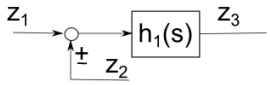	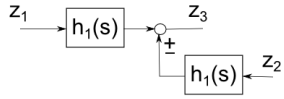
Moving a summation point in front of a block	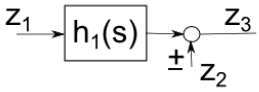	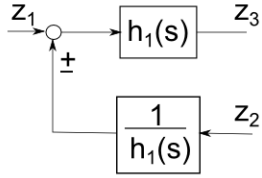
Moving a branch point behind a block	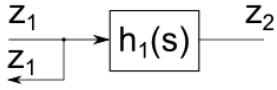	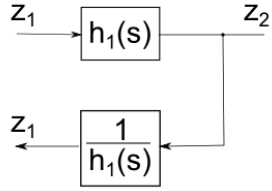
Moving a branch point in front of a block	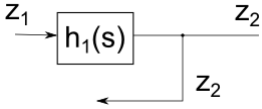	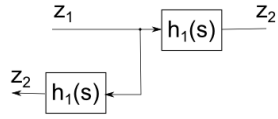
Eliminate a feedback loop	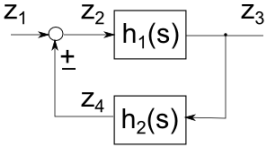	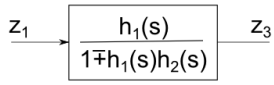

Table 2.1: Rules on how to reduce block diagrams [4]

2.10 APF Diagrams

An APF diagram is set up from the transfer function of a system. The APF diagram is used to conduct a stability analysis of the regulation system by examining phase angle and gain amplitude at different frequencies. The APF diagram shows the magnitude and phase shift of a frequency response.

Important aspects of an APF diagram:

1. Crossover frequency ω_c. The crossover frequency is the frequency at which the amplitude curve intersects the 0 dB line.
2. Gain margin Δk. Gain margin is the Δk from the 0dB line to the amplitude curve at the point where the phase curve is $-180°$.
3. Phase margin ψ. Phase margin is the distance between the phase curve and $-180°$, measured at the crossover frequency.

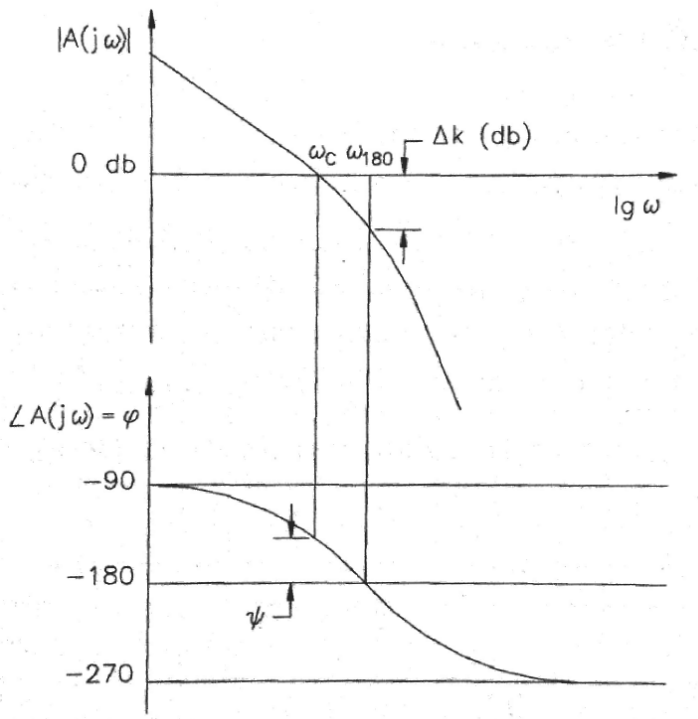

Figure 2.8: APF diagram [1]

According to the Nyquist stability criterion, the requirements for stability are the following [4]:

$$\angle h_0(j\omega_c) > -180^\circ \quad and \quad |h_0(j\omega_{180})| < 1 = 0dB \tag{2.26}$$

It is necessary to include a certain stability margin, hence the criteria become:

$$\psi \geq 45^\circ \quad and \quad \Delta k \geq 2 = 6dB \tag{2.27}$$

If the stability criteria is not met, the regulation system becomes unstable. One way to deal with that is to alter the regulation parameters. Furthermore, the closing time of the turbine valve can be increased. Another way is to introduce a free water surface closer to the turbine to decrease T_w. This is further described in the section below.

2.11 Water hammer and mass oscillations

When regulating the flow through a turbine, the water is either accelerated or decelerated. Due to this, pressure fluctuations in the penstock occur, and they can make regulating the turbine challenging. There are two types of pressure fluctuations that develop in a conduit;

1. Water hammer
2. Mass oscillations

Water hammer occurs when the volumetric flow through the turbine is regulated. For example at load rejection the water masses in the conduits are still moving when the turbine valve is closed. This will cause pressure to build up in front of the turbine, and shock waves will occur. Water and pipe are assumed elastic so that pressure surges propagate from the turbine with a speed equal to the speed of sound in water, which is $a \sim 1200m/s$. The pressure surge travels from the turbine to the nearest free water surface where it is reflected back to the turbine. The reflection time T_R of the water hammer is defined as the time it takes for the water hammer to travel from the turbine to the nearest free water surface and back to the turbine.

One way to minimize the effects of the pressure surges is to increase the closing time of the valve. Another way is to make the length of the waterway from the turbine to the nearest free water shorter by introducing a surge shaft. This however, creates a new problem, which is mass oscillations between the reservoir and the new free

water surface. These u-tube oscillations make the water oscillate in and out of the surge shaft, which makes the pressure in front of the turbine fluctuate as well. When explaining mass oscillations, the water is assumed incompressible.

Reducing the effects of water hammer is, as mentioned, one of the main reasons to implement a surge shaft in a hydropower system. Another advantage is that a surge shaft reduces the response time of the water masses. The response time T_w is described as the time it takes to accelerate the water masses between the nearest free water surface upstream of the turbine to the nearest free water surface downstream of the turbine from 0 to Q_0 [9]. It is defined as:

$$T_w = \frac{Q_0}{gH_0}\frac{L}{A} \tag{2.28}$$

Where Q_0 is the volumetric flow rate
g is the gravitational acceleration
H_0 is the hydraulic head
L is the length from the nearest free water surface to the turbine
A is the cross-sectional area of the tunnel or pipe

Equation 2.28 illustrates that introducing a free water surface near the turbine, and thus decreasing L, will decrease the response time as previously mentioned.

Pressure fluctuations in front of the turbine can have a negative effect on the stability of the regulation system. In hydropower systems with long conduits, the pressure change that follows a regulation will have a long way to travel, thus having a low frequency. When the frequency of the pressure surge becomes lower than the crossover frequency, the controller will start to regulate these. This will lead to further pressure change, which is undesirable. The main goal is that the pressure surges have a frequency higher than the crossover frequency to assure that the controller does not attempt to regulate these. It is therefore highly important to have a regulation system with the right parameters, so that stability is obtained.

2.11.1 The Thoma critical area

The surge shaft needs to be properly dimensioned to obtain stable u-tube oscillations and to prevent downsurge of air into the pipe or overspill. Thoma was the first to discover a requirement in surge shaft surface area. The Thoma critical area is defined as the minimum surface area of the surge shaft that gives stable u-tube oscillations

in a hydro system [9]:

$$A_{th} = \frac{LA}{2g\alpha H} \tag{2.29}$$

Where L is the length of the pipe
A is the pipe area
g is the gravitational acceleration
$\alpha = \frac{h_f}{V^2}$
H is the hydraulic head

As a safety margin, it is a common requirement that the minimum surface area has to be $A_{min} = 1.5 \cdot A_{th}$[9]. If the surge shaft surface area is below the required minimum, it can have severe consequences. If the water level falls below the floor of the surge shaft, air can escape into the penstock and this can be damaging to pipe, valves and machinery. It can also cause increased sediment transport. Furthermore, if an upsurge creates a water level in the surge shaft above the roof of the shaft, water can flow over the shaft, and this can be damaging to people and equipment in close proximity to the plant. Lastly, if the surface area is too small, the u-tube oscillations between reservoir and surge shaft can become unstable and grow larger and larger.

2.12 Surge shaft and air cushion surge chamber

The Thoma critical area is derived for surge shafts, but is valid for air cushion surge chambers by introducing an equivalent area A_{eq} and substituting for the shaft surface area [9].

$$A_{eq} = \frac{1}{\frac{1}{A_l} + \frac{nh_{p0}}{V_0}} \tag{2.30}$$

Where A_{eq} is the equivalent area
n is the adiabatic exponent = 1.4 for air
A_l is the area of the water surface in the air cushion
h_{p0} is the initial pressure in the air cushion

An air cushion surge chamber will in principle work in the same way as a surge shaft, however there are some essential differences. An air cushion surge chamber, unlike the surge shaft, does not need surface access (Figure 2.9). Instead of atmospheric pressure over the water surface there is a volume-dependent pressure. Hence the connecting tunnel between the air cushion surge chamber and the pipeline can be reduced. In addition, it eliminates the need for a pressure shaft, which results in

reduced length of the pipelines. These advantages will diminish the cost of the hydropower plant. However, the volume of an air cushion surge chamber needs to be much larger than that of the corresponding surge shaft.

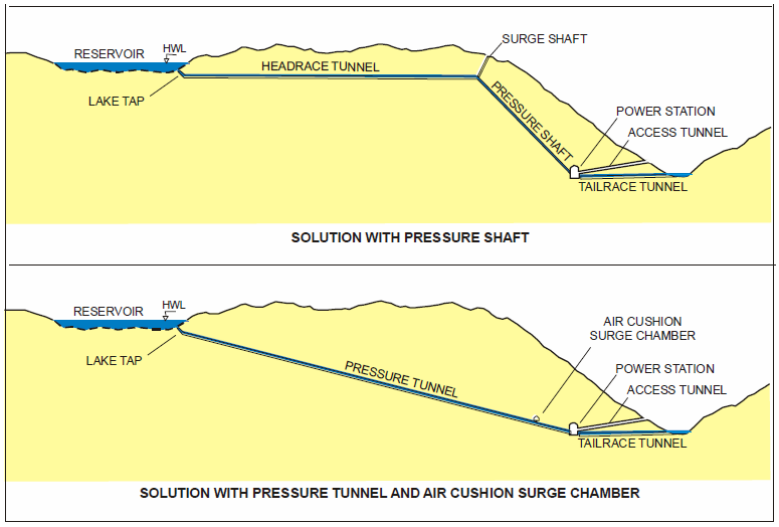

Figure 2.9: Surge shaft and air cushion surge chamber [2]

An air cushion surge chamber is a chamber filled with water and high-pressure air. As a rule of thumb, the pressure over the chamber must be larger than the air pressure within the chamber to avoid leakage of air [2]. This means that the quality of the rock is of high importance. So is the mapping of potential discontinuities in the rock mass. Ideally the rock should have low permeability so that the high-pressure air does not leak from the chamber, and the rock should be of about the same stiffness throughout the location around the air cushion surge chamber. Air leakage will lead to the need to refill the chamber with high-pressure air regularly, which is costly and should be minimized if possible.

One way to deal with air leakage is to drill holes in the rock over the chamber and inject cement or some sort of sealing compound. This prevents high-pressure air from leaking out of the chamber [2]. Another way that has proven effective is to drill holes over the chamber and pumping water into them, hence producing a water curtain over the chamber. The water curtain is connected to a water pump that keeps the pressure in the drill holes constant. This water curtain creates a higher pressure over than inside the air cushion surge chamber.

If the quality of the rock at the location of the power plant is poor, it is highly

important to have ways of dealing with it. The consequence of poor rock quality can be hydraulic jacking. This can happen if high-pressure air leaks out into the rock and then jacks the rock apart. It is therefore important that the air pressure inside the chamber is not too high. In addition, the chamber needs to be dimensioned right to avoid high-pressure air escaping into the penstock of the power plant. When air from the chamber escapes into the penstock, the air will experience reduced pressure and it will expand. This can cause a major blowout, which can cause damage to both pipe and inlet.

2.13 Frequency Regulation

The crossover frequency in an APF diagram for a system represents the limit at which frequencies the controller will function. All the pressure fluctuations with a lower frequency than the crossover frequency will be regulated. This normally includes the slow u-tube oscillations between reservoir and surge shaft. The pressure surges however, will normally have a higher frequency than the crossover frequency so that the controller does not attempt to regulate these. It is important to dimension a hydropower system in such a way that the elastic frequency is above the crossover frequency, so that these fluctuations will go about without any interference from the controller.

Stein‘s empirical equations are the foundation for obtaining the controller parameters [9]. For a PID controller they are the following:

$$k_p = 1.5 \cdot \frac{T_w}{T_a} \tag{2.31}$$

$$T_d = 3 \cdot T_w \tag{2.32}$$

$$T_N = 0.5 \cdot T_w \tag{2.33}$$

The controller parameters can be modified to obtained fast regulation whilst maintaining acceptable stability. Increasing k_p will lead to faster regulation, but also a less stable system. Decreasing k_p will lead to a more stable, but slower and more unresponsive system.

The P, I and D terms of the PID controller have different objectives:

- The proportional controller will calculate the error between power required in the grid and electric power generated by the plant. This value is multiplied by a constant, and the system is regulated.

- The integral controller is dependent on past errors and will look at the error over a period of time. Using only a P controller will not eliminate the error completely because the error is what drives the P controller. Only the integral parameter can eliminate the steady-state error.

- The derivative action is based on the slope of the error, but because it can cause instability it is often turned off.

2.14 Frequency balance in the electrical grid

In a power system there must be continuous balance between production and consumption. This balance is secured in several stages. The first step is when prices are fixed hour by hour the day before. This step secures planned balance hour by hour the next day. By this, production and consumption will be in balance in the planning phase. When it comes to running operation, this balance will change continuously. The frequency in the electrical grid is a measure of this momentary balance. When the consumption increases, the grid frequency will decrease. This is a signal to the generators to increase the production. And opposite, when the consumption decreases, the frequency will increase, thus giving a signal to the generators to decrease their production.

2.15 Design Criteria

Some of the design criteria that apply for a hydropower plant were presented above. The surge shaft surface area must be greater than the Thoma critical area to avoid unstable mass oscillations that grow larger and larger. The surge shaft has to be dimensioned in such a way that overspill to the surroundings is avoided. Surge shaft water level is also restricted by the maximum acceptable pressure in front of the turbine. This is because a high water level in the surge shaft will create a high pressure downstream of the shaft. In addition, if the surge shaft is underdimensioned, there is a risk of downsurge of air into the pipe. Downsurge of air from a surge shaft can cause damage to pipe and turbine, and it can lead to increased sediment transport. Downsurge of high-pressure air from an air cushion surge chamber can be even more damaging. It will cause a reduction in pressure of the escaped air, the air will expand and this can cause a blowout in the pipe, which can be highly destructive.

Highest assumed pressure increase in front of the turbine is dimensioning for a hydropower plant. The pressure change in front of the turbine should not exceed 20% of static pressure [10]. The dimensioning case for maximum pressure increase is a load rejection following a load acceptance in the most unfavorable stage, with maximum volumetric flow and highest regulated water level in the reservoir. This will cause the highest pressure increase in front of the turbine as well as the highest upsurge of water in the surge shaft. The maximum downsurge occurs at load acceptance, with lowest regulated water level in the reservoir.

The dimensioning criteria mentioned here are evaluated from an economical point of view in a project. If the pressure increase in front of the turbine appears to be higher than acceptable, the machinery and pipe dimensions can be increased. Another possibility is to increase closing time of the turbine valve. These measures will raise the costs of a project.

3 Analytical calculation

It is useful to conduct analytical calculations on the hydropower plant in question before commencing the simulations. By doing that, it is easier to get a sense of how the hydropower plant will operate and what to expect from simulations. In addition, one can see whether it is necessary with measures to increase stability, such as a surge shaft or an air cushion surge chamber. The equations used in the following section is from Torbjørn Nielsen's compendium [9].

3.1 Response time of the water masses

The response time of the water masses is the time it takes to accelerate the water masses between the nearest free water surface upstream of the turbine to the nearest free water surface downstream of the turbine from 0 to Q_0 [9].

$$T_w = \frac{Q_0}{gH} \Sigma \frac{L}{A} \tag{3.1}$$

Where T_w is the response time of the water masses
Q_0 is the volumetric flow
g is the gravitational acceleration
H is the hydraulic head
L is the length of the pipe
A is the pipe area

To obtain acceptable stability in a hydropower plant, T_w should be less than 1. T_w can be reduced by reducing the rate $\frac{L}{A}$, which is equivalent to introducing a free water surface closer to the turbine.

3.2 Head loss

The head loss in a hydropower system is energy lost to friction and singular losses. To calculate the head loss due to friction along a pipe, the Darcy-Weisbach equation is used.

$$h_f = \frac{fLV^2}{2gD_h} \tag{3.2}$$

Where h_f is head loss
f is the friction factor
L is the length of the pipe
V is the speed of the flow in the pipe
g is the gravitational acceleration
D_h is the hydraulic diameter

3.3 Closing time

Closing time T_L is the time it takes for the turbine valve to go from open to completely closed. A long closing time will reduce the water hammer occurring at load rejection. However, it will also lead to water being lost before the valve is closed completely. It is therefore important to find a balance between these when deciding on closing time.

If the reflection time of the water masses T_R is higher than T_L, the pressure increase in front of the turbine is assumed to happen instantaneously. This is because the valve goes from open to completely closed without the water masses being reflected back to the valve in the meantime. When T_R is less than T_L the pressure increase is not assumed to happen instantaneously, and pressure increase in front of the turbine will be lower than when T_R is higher than T_L. T_R is found as follows:

$$T_R = \frac{2L}{a} \tag{3.3}$$

Where T_R is the reflection time of the water masses
L is the length of the pipe
a is the speed of sound in water $\sim 1200\frac{m}{s}$

3.4 Pressure in front of the turbine

As previously mentioned there will be a change in pressure in front of the turbine because of deceleration or acceleration of the water masses in the pipeline when

the flow rate through the turbine is regulated. The pressure change in front of the turbine can be derived from the continuity equation and the equation of motion for the particular water string [9]. The waterway is assumed inelastic and loss-free, and $Q = v \cdot A$, so that the equation of motion becomes:

$$\frac{L}{gA}\frac{dQ}{dt} = \Delta H \tag{3.4}$$

And by assuming that the change in volumetric flow through the turbine is linear, the pressure change is dependent on the length and area of the pipeline as follows [9]:

$$\Delta h = \frac{\Delta Q}{T_L}\frac{L}{gA} \tag{3.5}$$

Where Δh is the change in pressure in mWC in front of the turbine
ΔQ is the change in volumetric flow
T_L is the closing time
L is the length of the pipe
g is the gravitational acceleration
A is the area of the pipe

Equation 3.5 holds for a rigid pipe and water column. The relation Joukowsky found for pressure change following an instant change [9], in mWC, is:

$$\Delta h = \frac{a\Delta v}{g} \tag{3.6}$$

When including elasticity effects, assuming $T_L > T_R$, and using the relations $T_R = \frac{2L}{a}$ and $\Delta Q = \Delta v \cdot A$ the equation become [9]:

$$\Delta h = \frac{a\Delta v}{g}\frac{T_R}{T_l} = 2\frac{\Delta Q}{T_L}\frac{L}{gA} \tag{3.7}$$

Equations 3.5 and 3.7 illustrate that the elasticity effects can double the pressure change in front of the turbine. A common constraint is that the pressure change in front of the turbine should not exceed 20% of static pressure [10].

3.5 Air cushion surge chamber

3.5.1 Thoma critical area

As previously mentioned, the Thoma critical area defines the minimum surge shaft surface area that is necessary to obtain stable u-tube oscillations.

$$A_{min} = 1.5A_{th} = 1.5\frac{LA}{2g\alpha H} \tag{3.8}$$

Where L is the length of the pipe
A is the pipe area
g is the gravitational acceleration
$\alpha = \frac{h_f}{V^2}$
H is the hydraulic head

The Thoma critical area is derived for surge shafts, but is valid for air cushion surge chambers by introducing an equivalent area A_{eq} and substituting for the shaft surface area. The equivalent area can also be used to calculate minimum air cushion volume needed:

$$A_{eq} = \frac{1}{\frac{1}{A_l} + \frac{nh_{p0}}{V_0}} \tag{3.9}$$

Or rearranged:

$$V_0 = \frac{nh_{p0}}{\frac{1}{A_{eq}} - \frac{1}{A_l}} \tag{3.10}$$

Where A_{eq} is the equivalent area
n is the adiabatic exponent = 1.4 for air
A_l is the area of the water surface in the air cushion
h_{p0} is the initial pressure in the air cushion

h_{p0} is the initial pressure in the air cushion and is found from the equation:

$$H + h_{atm} = h_{p0} + WL_{sh} + h_f \tag{3.11}$$

Where H is the hydraulic head
h_{atm} is the atmospheric pressure = $10mWC$

WL_{sh} is the water level of the water surface area of the shaft
h_f is the head loss

3.5.2 Amplitude of u-tube oscillations

The maximum up- and downsurge following a change in volumetric flow can be derived from the equation of motion for the u-tube between reservoir and surge shaft, when assuming no loss, and the equation of continuity for the connection between tunnel and shaft [9]. Introducing the equivalent area makes the equation valid for an air cushion surge chamber.

$$\pm\Delta h = \pm\Delta Q\sqrt{\frac{L/A}{gA_{eq}}} \tag{3.12}$$

Where Δh is the maximum and minimum amplitude of the u-tube oscillations
ΔQ is the change in volumetric flow
L is the length of the pipe
A is the pipe area
g is the gravitational acceleration
A_{eq} is the equivalent area

Equation 3.12 does not account for loss. The upsurge and downsurge can be corrected for head loss in the manner illustrated below [9].

$$\Delta h_{up} = \Delta Q\sqrt{\frac{L/A}{gA_{eq}}} + \frac{1}{3}h_f \tag{3.13}$$

Where h_f is the head loss of stationary flow before load rejection, and Δh_{up} is the upsurge.

$$\Delta h_{down} = -\Delta Q\sqrt{\frac{L/A}{gA_{eq}}} - \frac{1}{9}h_f^0 \tag{3.14}$$

Where h_f^0 is the head loss of stationary flow before load acceptance, and Δh_{down} is the downsurge.

However, the air cushion consists of high-pressure air and not air at atmospheric pressure. The following steps can be used to find the actual up- and downsurge Δz in the air cushion [11].

First finding the water volume and then the up- and downsurge:

$$V_{water} = \Delta h A_{eq} \tag{3.15}$$

$$\Delta z = \frac{V_{water}}{A_l} \tag{3.16}$$

3.5.3 Natural frequency of u-tube oscillations

The natural frequency of the u-tube oscillations between air cushion surge chamber and reservoir can be expressed as [9]:

$$\omega = \sqrt{\frac{g}{A_{eq} \cdot L/A}} \tag{3.17}$$

Where ω is the natural frequency
g is the gravitational acceleration
A_{eq} is the equivalent area
L is the length of the pipe
A is the pipe area

And the period is

$$T = \frac{2\pi}{\omega} \tag{3.18}$$

If an equivalent area that is less than the Thoma critical area is used, the amplitude can become infinitely large and the oscillations will become unstable.

4 Herand power plant

Herand power plant will be located in Jondal municipality in Hordaland. The hydropower plant will utilize the hydraulic head between Storelvi, at 527 meters above sea level, and Trå, at 90 meters above sea level (Figure 4.1). The power plant will be situated at Trå, which will give a gross head of 437 meters. The inlet will be located right below Fodnastølsvatnet, which will be left untouched, however the power plant will utilize its ability of self-regulation. This will be the only regulation as Herand will be a run-of-river power plant. The conduits at Herand power plant will consist of 2600 meters of buried pipes and the turbine type will be a vertical Pelton. Herand will have a generator of 27MVA, with a power production of 23.4MW. Figure 4.2 shows the altitude profile of the terrain at the location of the power plant.

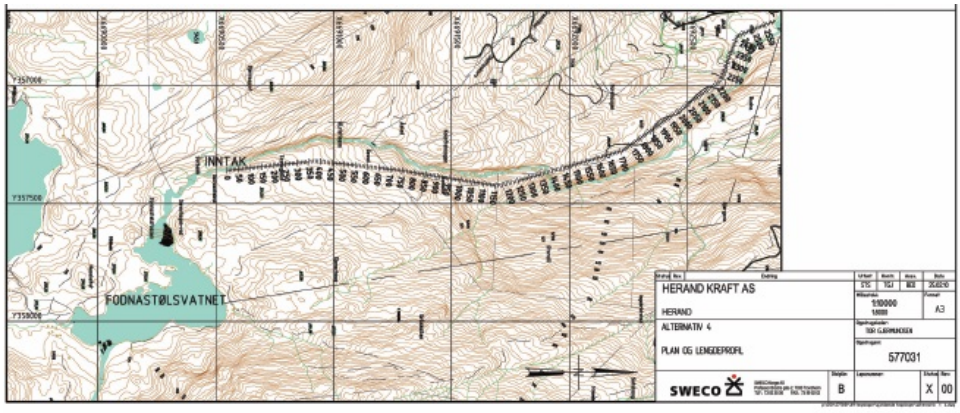

Figure 4.1: Altitude profile no.2 [3], larger scale of this figure is included in Appendix D

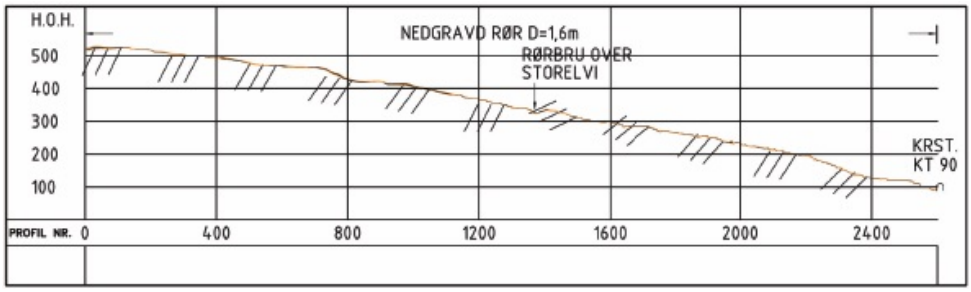

Figure 4.2: Altitude profile no.1 [3]

The layout of Herand power plant is illustrated in Figure 4.3, and the parameters are presented below.

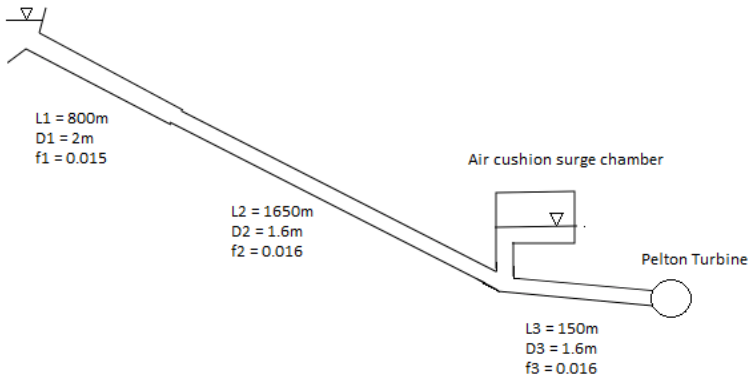

Figure 4.3: Herand power plant layout

4.1 Penstock

The pipeline at Herand power plant will be 2600 meters long, with a hydraulic height of 437 meters. The first 800 meters are GRP pipes, which stands for Glassfibre Reinforced Polystyren. The remaining 1800 meters of pipelines are ductile iron pipes. The pipe parameters are presented in Table 4.1.

		GRP pipes	Ductile iron pipe 1	Ductile iron pipe 2
Length	L	800 [m]	1650 [m]	150 [m]
Diameter	D	2 [m]	1.6 [m]	1.6 [m]
Friction factor	f	0.015 [-]	0.016 [-]	0.016 [-]

Table 4.1: Pipe Parameters

4.2 Turbine

The turbine type that will be used at Herand is a vertical Pelton. The power plant data are presented in Table 4.2.

	Parameter	Value	
Rated discharge	Q_r	5.14	$[\frac{m^3}{s}]$
Hydraulic head	H	437	[m]
Time constant for angular masses	T_a	6	[s]
Turbine discharge, max	Q_{max}	6.35	$[\frac{m^3}{s}]$
Turbine discharge, min	Q_{min}	0.15	$[\frac{m^3}{s}]$

Table 4.2: Power plant data

4.3 Air cushion surge chamber

The dimensions of Herand's air cushion surge chamber were obtained from analytical and numerical calculations, and will be presented later in this paper.

4.4 Controller

The controller parameters were calculated based on Stein's empirical formulas (Section 2.13). However, these equations are just a starting point when finding the optimal controller settings. The parameters will be adjusted to obtain fast regulation whilst still maintaining a stable control system.

	Parameter	Value
Gain	k_p	0.022
Integral time	T_i	0.264
Derivation time	T_N	0.044
Closing time	T_L	10 [s]

Table 4.3: Controller parameters based on Stein's empirical formulas

4.5 Requirements

Herand power plant is planned to have a generator of 27MVA and will therefore fall under the requirements of frequency regulation set by the Norwegian Transmission System Operator (TSO), which is Statnett. They have developed a guide to the requirements for power systems called FIKS [7], which amongst other things states that all generators above 10MVA must have frequency regulation and be able to operate in an isolated grid. Below is an extract from the document.

"*Satisfactory stability is characterized by phase margin being in the interval between* 25° *and* 35°*, and gain margin being in the range between 3dB to 5dB at full-load operation of an ohmic network with a constant voltage.*" [7]

However, the conditions at Herand will present a challenge when it comes to stability and frequency regulation, both technically and economically. The challenges for Herand when it comes to meeting the requirements set by FIKS are related to the challenging topography at the location of the power plant. Another reason is that Herand is a run-of-river hydropower plant where the inflow at any given time will decide production. The only regulation Herand will have is the natural regulation of the Fodnastølsvatnet, where the inlet is located. This means that Herand will only receive the natural flow of water coming from the lake, and will have limited ability to increase production beyond this inflow. The reason why Herand must have regulation abilities is that the plant must be able to reduce production, and potentially shut down completely when it loses connection with the central grid. If not, too much power could be transferred to an area with little or no load, hence risking overspeed of the generator.

Another challenge facing Herand due to topography is concerning methods for reducing water hammer effects and reducing response time of the water masses. A surge shaft was not feasible, so an air cushion surge chamber was introduced.

5 Methodology

A stability analysis was conducted on Herand power plant both with and without an air cushion surge chamber by the means of a frequency response analysis. A frequency response analysis involves applying a sinusoidal signal at a frequency as input to the system and investigating the system's output at the same frequency. This is repeated for all relevant frequencies. Hence characterizing the dynamics of the system [4]. The response can be shown in a Bode plot, which graphically shows the magnitude and phase of the system's response of a sinusoidal input. The magnitude is shown in decibel (dB) as a function of frequency, and the phase is shown in degrees or radians as a function of frequency. The frequency is measured in Hertz (Hz) on a logarithmic scale.

To conduct a frequency response analysis, a block diagram of Herand power plant was inserted into Simulink. Simulink is a computer program used to model and simulate dynamic systems. It is integrated with Matlab. Block diagrams are developed in Simulink, and are based on differential equations of the elements of the physical system in question. Simulink solves mathematical models, such as the mathematical model of a hydropower system, that are too complicated, or undesirable, to solve analytically.

5.1 Without an air cushion surge chamber

The complete block diagram for Herand power plant without an air cushion surge chamber becomes as illustrated in Figure 5.1. The block diagram was inserted into the computer program Simulink, and the parameters were given values in Matlab (Appendix C). After that, the linear analysis was run in Simulink. Simulink then created a Bode diagram, which was used to analyze stability of Herand power plant.

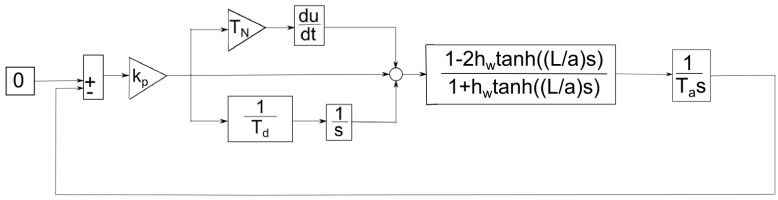

Figure 5.1: Block diagram of Herand including the elastic property of the penstock

The stability analysis conducted on Herand power plant without an air cushion surge chamber included the elastic property of the penstock. The pressure fluctuations in a long penstock following a regulation of volumetric flow through the turbine will have an effect on stability. Simulink created a Bode diagram displaying the pressure fluctuations when the elastic property of the penstock was included in the model.

The term tanh could not be inserted into Simulink, so the transfer function involving tanh was rewritten in terms of sinh and cosh, and these terms were then expanded based on common expansion rules [12].

$$\tanh(\frac{L}{a}s) = \frac{\sinh(\frac{L}{a}s)}{\cosh(\frac{L}{a}s)} \tag{5.1}$$

Expansion of $\sinh(x)$ and $\cosh(x)$

$$\sinh(x) = x + \frac{x^3}{3!} + \frac{x^5}{5!} + \frac{x^7}{7!} + ... \tag{5.2}$$

$$\cosh(x) = 1 + \frac{x^2}{2!} + \frac{x^4}{4!} + \frac{x^6}{6!} + ... \tag{5.3}$$

The reason why the expansion of $\tanh(x)$ was not used directly, is that the area of validity for x is $|x| < \frac{\pi}{2}$, whilst $\sinh(x)$ and $\cosh(x)$ are valid for all x.

5.2 With an air cushion surge chamber

Introducing an air cushion surge chamber changes the physical system. In the simulations, the pipe from the air cushion surge chamber was assumed elastic. The pipe from the inlet to the air cushion surge chamber on the other hand, was assumed

inelastic. So was the actual chamber. The complete block diagram became as illustrated in Figure 5.2 when the complete system was included and assumed rigid, and $K_t = \frac{fLV_0^2}{2gDH_0}$.

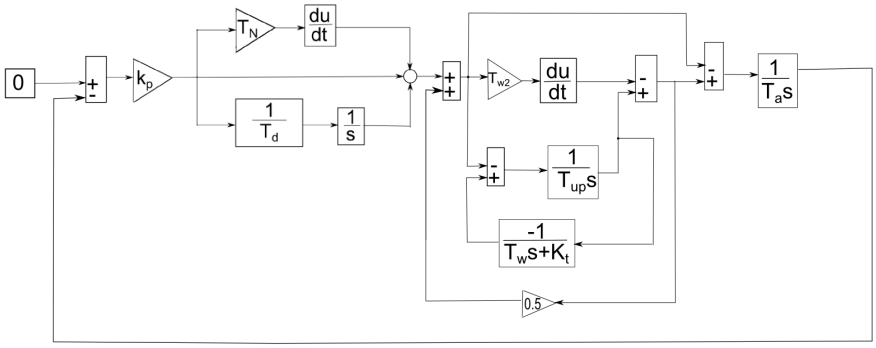

Figure 5.2: Block diagram of Herand with an air cushion surge chamber assuming rigid penstock

The simulation of Herand power plant with an air cushion surge chamber was conducted in two phases. First finding the frequency of the mass oscillations when assuming a rigid penstock, and then finding the frequency of the pressure fluctuations including the elastic property of the penstock.

5.2.1 Finding the frequency of mass oscillations

The mass oscillations occur between the inlet and the air cushion surge chamber after regulation of volumetric flow through the turbine. The air cushion volume is important in this respect, however the penstock from the air cushion surge chamber and to the turbine is not of importance when examining mass oscillations. The frequency of the mass oscillations was found by ignoring the elasticity effects of the penstock (Figure 5.2).

5.2.2 Finding the frequency of pressure fluctuations

The pressure fluctuations in front of the turbine was found by including the elasticity effects of the penstock. In this respect, the system further up from the penstock connected to the turbine is not of importance. This is because the pressure fluctuations originate in front of the turbine and will be reflected back from the nearest free water surface, which at Herand will be the air cushion surge chamber. The simulated system therefore became as illustrated in Figure 5.1, which is the same system as

Herand without an air cushion surge chamber. The difference is the length L, which here was 150m.

By combining these two methods, the stability analysis of the complete system was obtained.

6 Methodology for analytical approach

The method presented in the paper "*Cavitation and dynamic problems*" by Torbjørn K. Nielsen [8] is an analytical approach for obtaining APF diagrams. The method applies some of the theory presented in Chapter 2 of this paper. The block diagram of a system is used to obtain the transfer function. The method includes the theory of the elastic property of a penstock. The method uses control theory to obtain equations for the amplitude and phase angle from a transfer function. For a general transfer function [4]

$$A(s) = A(j\omega) = \frac{(1 + T_1 s)(1 + T_2 s)}{(1 + T_3 s)(1 + T_4 s)} \tag{6.1}$$

The amplitude is [4]:

$$|A(j\omega)| = \sqrt{\frac{(1 + (\omega T_1)^2)(1 + (\omega T_2)^2)}{(1 + (\omega T_3)^2)(1 + (\omega T_4)^2)}} \tag{6.2}$$

And the phase angle is [4]:

$$\angle A(j\omega) = \arctan(\omega T_1) + \arctan(\omega T_2) - \arctan(\omega T_3) - \arctan(\omega T_4) \tag{6.3}$$

By rewriting tanh, the method presents the amplitude and phase angle for a complete hydropower system including PID controller, waterway and turbine inertia. See the paper for full derivation [8]. The results are:

The complete transfer function for the rigid system is:

$$A(j\omega) = \frac{1}{b_t T_d T_a} \frac{(1+T_d s)(1+T_N s)}{s^2} \frac{1-T_w s}{1+0.5T_w s} \tag{6.4}$$

Where $b_t = \frac{1}{k_p}$

Amplitude:

$$A(j\omega) = \frac{1}{b_t T_d T_a} \sqrt{\frac{(1+(\omega T_d)^2)(1+(\omega T_N)^2)}{\omega^4} \frac{1+(\omega T_w)^2}{1+(0.5\omega T_w)^2}} \tag{6.5}$$

Phase angle:

$$\angle A(j\omega) = \arctan(\omega T_d) + \arctan(\omega T_N) - \arctan(\omega T_w) - \arctan(0.5\omega T_w) - \pi \tag{6.6}$$

The complete system for the elastic system is:

$$A(j\omega) = \frac{1}{b_t T_d T_a} \frac{(1+T_d s)(1+T_N s)}{s^2} \frac{1-2h_w \tanh(\frac{L}{a}s)}{1+h_w \tanh(\frac{L}{a}s)} \tag{6.7}$$

Amplitude:

$$A(j\omega) = \frac{1}{b_t T_d T_a} \sqrt{\frac{(1+(\omega T_d)^2)(1+(\omega T_N)^2)}{\omega^4} \frac{1+(2h_w \tan(\frac{L}{a}s))^2}{1+(h_w \tan(\frac{L}{a}s))^2}} \tag{6.8}$$

Phase angle:

$$\begin{aligned} \angle A(j\omega) = \arctan(\omega T_d) + \arctan(\omega T_N) - \arctan(2h_w \tan(\frac{L}{a}\omega)) \\ - \arctan(h_w \tan(\frac{L}{a}\omega)) - \pi \end{aligned} \tag{6.9}$$

The APF diagrams can be generated by inserting the equation set into an analytical solver, such as Excel.

7 Results

The results form the analytical calculations, the numerical simulations and the analytical approach to obtaining Bode plots are presented in this section.

7.1 Analytical results

In this section the results of the analytical calculations are presented. The equations are discussed in Chapter 3, and here they will only be presented. The complete calculations are found in Appendix B. The volumetric flow used in the calculations was the rated value. This value was found from the rated power, which is $P_r = \frac{P_{max}}{1.2} = 19.75MW$:

$$Q_r = \frac{P_r}{\eta\rho g(H - h_f)} = 5.14m^3/s \tag{7.1}$$

7.1.1 Response time of the water masses

The response time of the water masses when the air cushion surge chamber was not included became:

$$T_w = \frac{Q_0}{gH}(\frac{L_1}{A_1} + \frac{L_2}{A_2}) = 1.38s \tag{7.2}$$

Since $T_w > 1$, an air cushion surge chamber is needed to obtain stability. The response time of the water masses when the air cushion surge chamber is included was:

$$T_w = \frac{Q_0}{gH}\frac{L_3}{A_3} = 0.089s \tag{7.3}$$

7.1.2 Head loss

The head loss in the system was:

$$h_f = \frac{fLV^2}{2gD} = 6.81mWC \tag{7.4}$$

Where the unit mWC is meter water column.

7.1.3 Closing time and reflection time

The closing time of the turbine valve was:

$$T_L = 10s \tag{7.5}$$

And the reflection time was:

$$T_R = \frac{2L_3}{a} = 0.25s \tag{7.6}$$

Since $T_L > T_R$, the closing of the valve was not assumed to happen instantaneously.

7.1.4 Pressure in front of the turbine

The pressure change in front of the turbine at load rejection without an air cushion surge chamber was:

$$\Delta h = 2\frac{\Delta Q}{T_L}\frac{L}{gA} = 135.5mWC \tag{7.7}$$

When including an air cushion surge chamber, the pressure change in front of the turbine became:

$$\Delta h = 2\frac{\Delta Q}{T_L}\frac{L}{gA} = 7.8mWC \tag{7.8}$$

7.1.5 Thoma critical area

The Thoma critical area that will assure stable u-tube oscillations was:

$$A_{min} = A_{eq} = 1.5A_{th} = 1.5\frac{LA}{2g\alpha H} = 0.887m^2 \tag{7.9}$$

The volume of the air cushion became:

$$V_0 = \frac{nh_{p0}}{\frac{1}{A_{eq}} - \frac{1}{A_l}} = 527.6m^3 \tag{7.10}$$

Where

$$h_{p0} = H + h_{atm} - WL_{sh} - h_f = 437 + 10 - 20 - 6.81 = 420.2mWC \tag{7.11}$$

And $A_l = 80m^2$, so that the height of the air cushion became:

$$h_{aircush,init} = \frac{V_0}{A_l} = 6.6m \tag{7.12}$$

From [13], the total volume of the air cushion surge chamber is defined as:

$$V_{rock} = 1.35V_0 = 712.26m^3 \tag{7.13}$$

Which means that the initial water volume was $184.66m^3$, and the water surface heigh in the chamber was $h_{water,init} = \frac{184.66m^3}{80m^2} = 2.31m$.

7.1.6 Amplitude of u-tube oscillations

The upsurge in the air cushion surge chamber was calculated to be:

$$\Delta h_{up} = \Delta Q\sqrt{\frac{L/A}{gA_{eq}}} + \frac{1}{3}h_f = 59.4m \tag{7.14}$$

And the downsurge was:

$$-\Delta h_{down} = -\Delta Q\sqrt{\frac{L/A}{gA_{eq}}} - \frac{1}{9}h_f^0 = -58m \tag{7.15}$$

However, the air cushion is filled with high-pressure air. The volume and the upsurge was therefore:

$$V_{water} = \Delta h_{up}A_{eq} = 52.7m^3 \tag{7.16}$$

$$\Delta z_{up} = \frac{V_{water}}{A_l} = \frac{52.7m^3}{80m^2} = 0.66m \tag{7.17}$$

The participating volume and the downsurge became:

$$V_{water} = \Delta h_{down}A_{eq} = -51.5m^3 \tag{7.18}$$

$$\Delta z_{down} = \frac{-51.5m^3}{80m^2} = -0.64m \tag{7.19}$$

7.1.7 Natural frequency of u-tube oscillations

The natural frequency of the u-tube oscillations was:

$$\omega = \sqrt{\frac{g}{A_{eq}L/A}} = 0.1014rad/s \tag{7.20}$$

Which in Hertz is $\frac{0.1014}{2\pi} = 0.016Hz$.

And the period was:

$$T = \frac{2\pi}{\omega} = 62s \tag{7.21}$$

7.2 Numerical results

In this section the results from the simulations are presented. As previously mentioned, the simulations were conducted with three different models; elastic system without air cushion surge chamber, elastic system from air cushion surge chamber to turbine, and rigid system with air cushion surge chamber.

The controller parameters were decided during simulations based on obtaining a fast, but stable regulation system and getting amplitude gain and phase angle within the required values (Section 2.13). Increasing k_p will move the magnitude graph to the right, and thus moving the crossover frequency to a higher frequency. The system will obtain faster regulation, however it can become more unstable. Likewise, if k_p is decreased, the system will be stable, but it can become too slow and unresponsive. The final controller parameters are presented in the caption for each figure.

7.2.1 Without an air cushion surge chamber

The elastic property of the penstock was included in the simulations of Herand power plant without an air cushion surge chamber. As seen in Figure 7.1, elastic waves was shown when including elastic effects. The crossover frequency was 0.35Hz. Figure 7.1 shows that the elastic frequencies start from 0.12Hz. $\Delta k = 22dB$, and phase margin was 43 degrees.

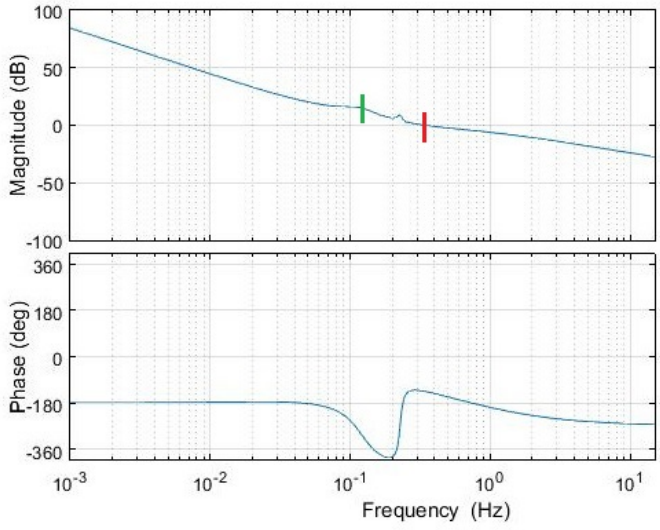

Figure 7.1: Elastic system without an air cushion surge chamber, $k_p = 12$, $T_d = 3$, $T_N = 0$

The system was also simulated with other controller parameters (Figure 7.2) to check whether that could enhance stability. The crossover frequency was then 0.045Hz. The elastic frequency started from 0.117Hz. $\Delta k = 0.75dB$, and phase margin was 1 degree.

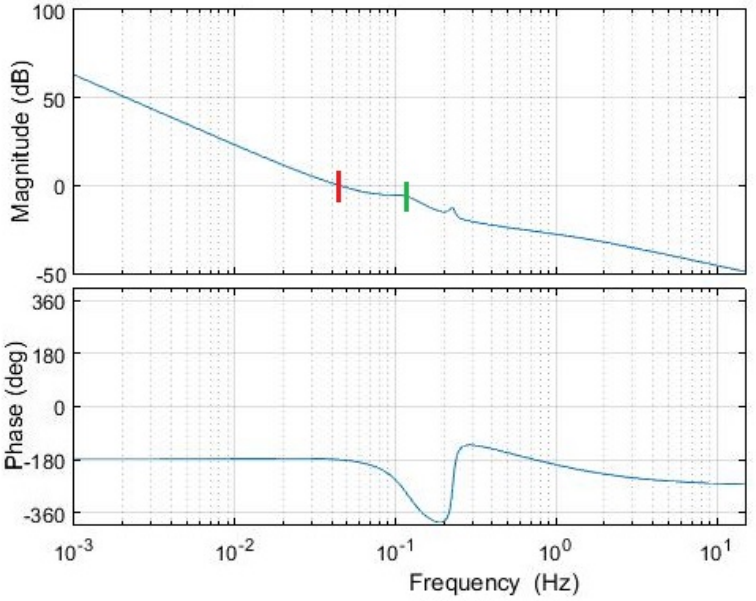

Figure 7.2: Elastic system without an air cushion surge chamber, $k_p = 1$, $T_d = 3$, $T_N = 0$

In some of the simulations, like the ones above, the phase offsets was not adjusted to -180 degrees in Simulink. This was manually fixed for the concerning graphs.

7.2.2 With an air cushion surge chamber

The simulations with an air cushion surge chamber were done in two phases, as explained in Chapter 5.

Case 1 - Rigid

The complete system including an air cushion surge chamber was simulated, but the penstock was assumed rigid. Figure 7.3 shows the frequency of the mass oscillations that occur between the inlet and the air cushion surge chamber. The Bode diagram shows that the crossover frequency was 0.325Hz. The frequency of the mass oscillations was 0.015Hz.

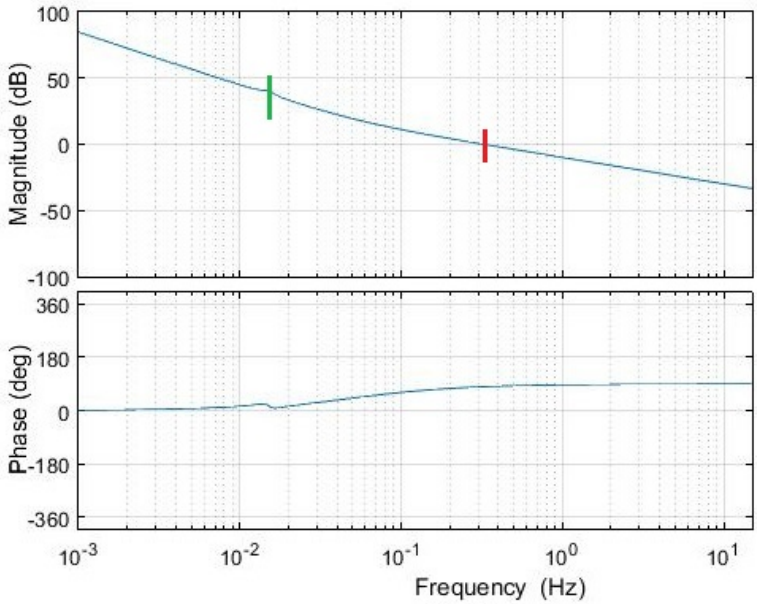

Figure 7.3: Rigid system with air cushion surge chamber, $k_p = 12$, $T_d = 3$, $T_N = 0$

Case 2 - Elastic

Only the pipe leading down from the air cushion surge chamber to the turbine was included in the simulations for finding the frequencies of the pressure fluctuations. This was because the fluctuations occur in that pipe segment, and the mass oscillations occurring upstream of the air cushion surge shaft was simulated in Case 1. The pipe was assumed elastic.

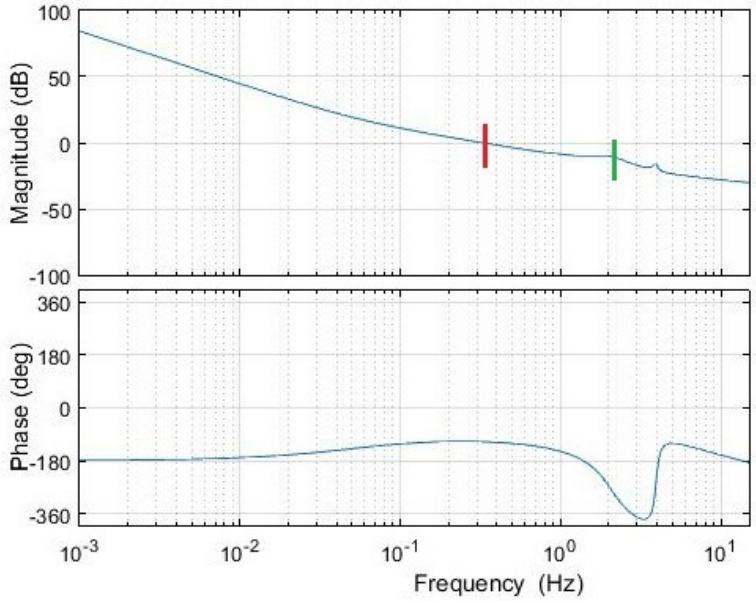

Figure 7.4: Elastic system with air cushion surge chamber, $k_p = 12$, $T_d = 3$, $T_N = 0$

The Bode diagram shows that the crossover frequency was 0.325Hz. The frequency of the pressure fluctuations were above 2Hz. The phase margin was 65 degrees, and Δk was 9.8dB.

7.3 Other operating points

The simulations above were conducted with the turbine's rated discharge, which is $5.14m^3/s$. The stability was also analyzed with maximum discharge, which is $6.35m^3/s$.

The downsurge of high-pressure air from the air cushion surge chamber to the pipe must be avoided at all operating points. At maximum volumetric flow through the turbine, the downsurge became:

$$-\Delta h_{down} = -\Delta Q \sqrt{\frac{L/A}{gA_{eq}}} - \frac{1}{9} h_f^0 \tag{7.22}$$

$$-\Delta h_{down} = -6.35m^3/s \sqrt{\frac{\frac{800m}{\pi m^2} + \frac{1650m}{2.0106m^2}}{9.81m/s^2 0.887m^2}} - \frac{1}{9} 10.4m = -71.7m \tag{7.23}$$

Which became:

$$V_{water} = \Delta h_{down} A_{eq} = -71.7m0.887m^2 = -63.6m^3 \tag{7.24}$$

$$\Delta z_{down} = \frac{-63.6m^3}{80m^2} = -0.7575m \tag{7.25}$$

The downsurge of water was $0.7575m$.

The numerical simulation of the pipe from the air cushion surge chamber to the pipe with maximum discharge is shown in Figure 7.5. The crossover frequency was 0.328Hz. The frequency of the pressure surge was 1.75Hz. $\Delta k = 9dB$, and phase margin was 61 degrees.

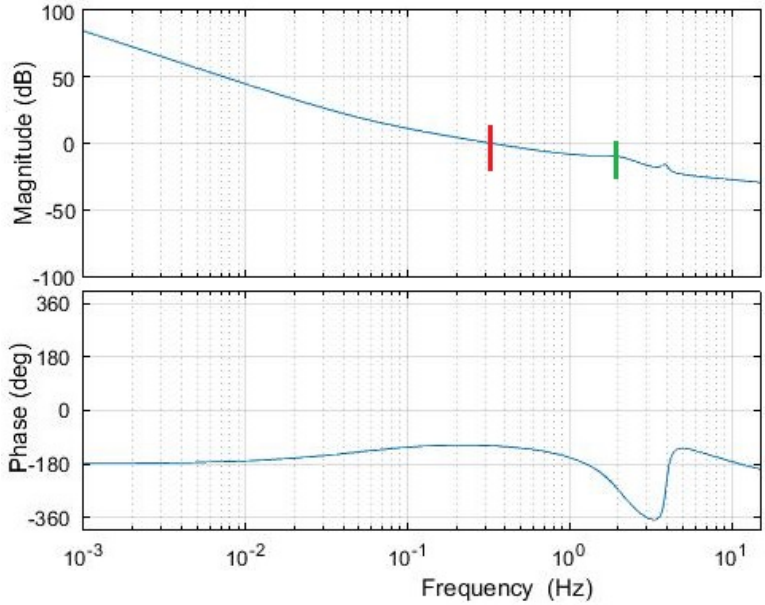

Figure 7.5: Elastic system, maximum discharge, $k_p = 12$, $T_d = 3$, $T_N = 0$

7.4 Verification and Comparison

The analytical approach to obtaining Bode plots was described in Chapter 6. Excel was used to obtain the Bode plot for the analytical approach. The analytical approach was conducted to verify the numerical simulations from Simulink, and to examine whether the two methods provide the same results.

7.4.1 Without an air cushion surge chamber

The elastic property of the penstock was included in both the analytical method and the simulations so that the Bode plots show the elastic frequencies. The Bode plots for Herand power plant without an air cushion surge chamber from the numerical approach and from simulation are presented in Figures 7.6 and 7.7. The results from the analytical approach are graphed to the left, and the simulation results are to the right.

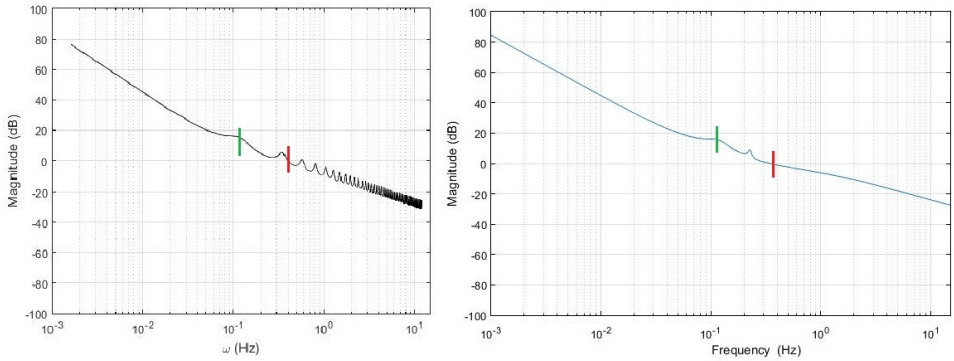

Figure 7.6: Bode plot (magnitude) from analytical approach, without air cushion surge chamber, $k_p = 12$, $T_d = 3$, $T_N = 0$

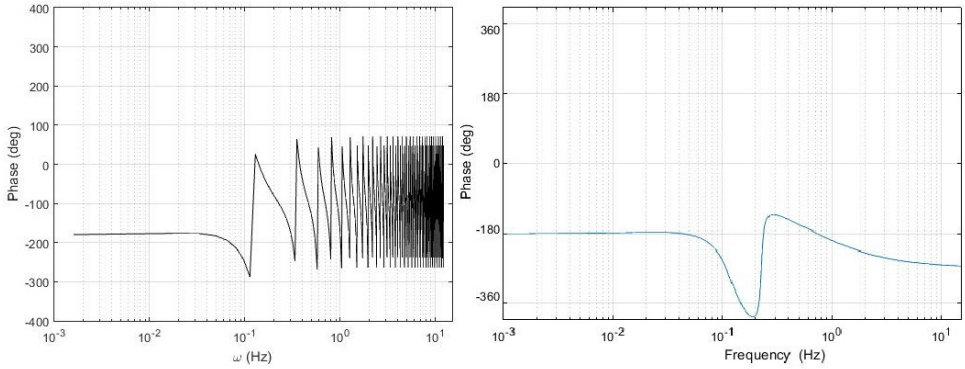

Figure 7.7: Bode plot (phase) from analytical approach, without air cushion surge chamber, $k_p = 12$, $T_d = 3$, $T_N = 0$

7.4.2 With an air cushion surge chamber

Simulation results of Herand power plant with an air cushion surge chamber and including elasticity effects were compared to the results from the numerical approach.

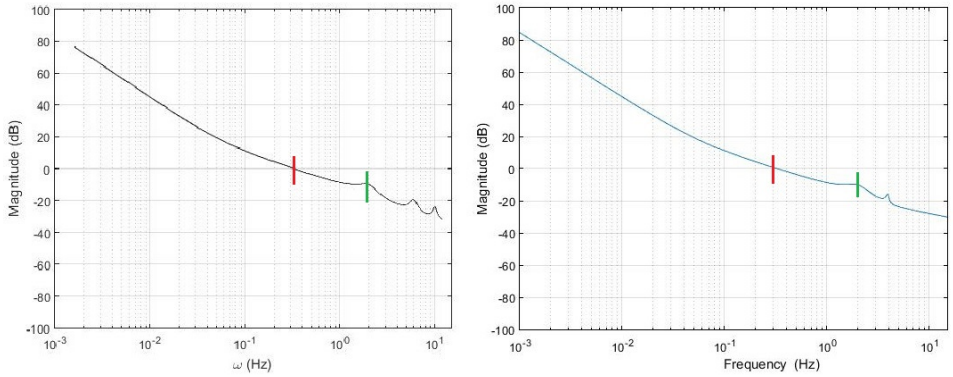

Figure 7.8: Bode plot (magnitude) from analytical approach, with air cushion surge chamber, $k_p = 12$, $T_d = 3$, $T_N = 0$

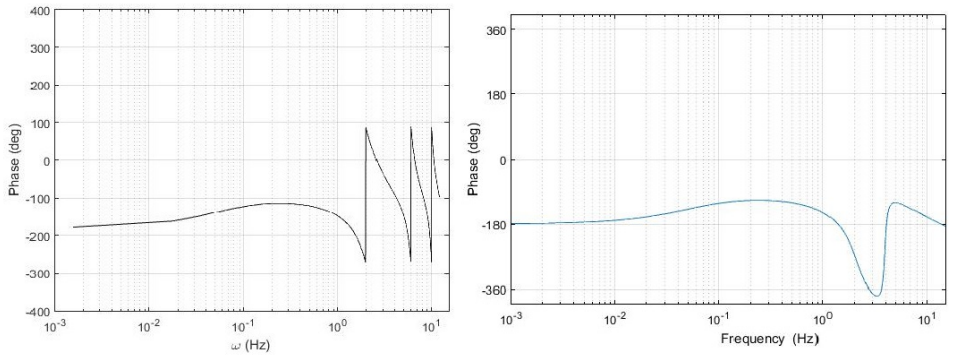

Figure 7.9: Bode plot (phase) from analytical approach, with air cushion surge chamber, $k_p = 12$, $T_d = 3$, $T_N = 0$

8 Discussion

Some of the results are presented below in Tables 8.1 and 8.2. The other results that are discussed in this chapter will be referred to.

		Without air cushion surge chamber	With air cushion surge chamber
Response time	T_w	1.38 [s]	0.089 [s]
Pressure in front of the turbine	Δh	135.5 [mWC]	7.8 [mWC]
Volume of air cushion	V_0	-	527.6 $[m^3]$
Total volume of air cushion surge chamber	V_{rock}	-	712.26 $[m^3]$
Amplitude of u-tube oscillations	Δz_{up}	-	0.66 [m]
Amplitude of u-tube oscillations	Δz_{down}	-	-0.64 [m]

Table 8.1: Results from analytical calculations

		Without air cushion surge chamber	With air cushion surge chamber
Crossover frequency	ω_c	0.35 [Hz]	0.325 [Hz]
Frequency of pressure fluctuations	ω_p	0.12 [Hz]	2 [Hz]
Frequency of mass oscillations	ω_m	-	0.015 [Hz]
Phase margin at crossover frequency	Ψ	43 [deg]	65 [deg]
Gain margin	Δk	22 [dB]	9.8 [dB]

Table 8.2: Results from numerical simulations

8.1 Response time

The calculated T_w shows that Herand power plant needs to implement a measure for enhancing stability in its conduit (Table 8.1), because the stability requirement for T_w is that it has to be < 1. When an air cushion surge shaft was implemented $150m$ upstream of the turbine, T_w was 0.089s. This indicates that Herand power plant will obtain acceptable stability when introducing an air cushion surge chamber. The fact that T_w is much smaller than 1, indicates that the location of the air cushion surge chamber suggested in this paper is not restrictive. Thus, if the optimal location of the air cushion surge chamber later proves to be further up the pipe, this will not, based on the analytical calculations, create a problem. However, T_w is not a sufficient criteria for stability when the penstock is long and the elastic property is included. Therefore, a stability analysis that includes the elastic property was conducted.

8.2 Pressure in front of the turbine

The static pressure in front of the turbine is 437mWC. The pressure increase at load rejection for the conduits without an air cushion surge chamber was 135.5mWC (Table 8.1). That is 31% of 437 and will therefore cause a significant pressure increase in front of the turbine. A common constraint is that the pressure change in front of the turbine should not exceed 20% of static pressure. However, introducing a new free water surface closer to the turbine reduced the pressure increase occurring in front of the turbine at load rejection to 7.8mWC (Table 8.1), which is 1.7% of static pressure. This will have significance for dimensioning of pipe, valves and machinery. These must be dimensioned to withstand pressure fluctuations in the system at all scenarios. By implementing an air cushion surge chamber, the dimensions of pipe, valves and machinery can be reduced compared to without an air cushion surge chamber, and thus reducing costs.

8.3 Dimensions of air cushion surge chamber

The dimensions of the air cushion surge chamber were given by the analytical calculations. The Thoma critical area is the minimum surface area that gives stable u-tube oscillations, and the air cushion volume of $527.6m^3$ was used in the numerical simulations. The total volume of the chamber was $712.26m^3$, and it lies 150m upstream of the turbine. Equations 7.17 and 7.19 show that the system will not experience overspill of water or intake of high-pressure air from the air cushion surge chamber into the pipe. This is because the maximum up- and downsurge following a load rejection or load acceptance respectively, will not grow beyond the dimensions of the air cushion surge chamber. The calculations with maximum discharge show that

up- and downsurge is avoided also at that operating point, and thus at all operating points.

8.4 Numerical results without air cushion surge chamber

The elastic property of the penstock was included in the simulations of Herand power plant without an air cushion surge chamber. As illustrated in Figure 7.1, elastic waves will occur when including elastic effects. The crossover frequency was 0.35Hz. At frequencies above the crossover frequency, the controller will not attempt to regulate fluctuations in pressure. However, Figure 7.1 shows that the elastic frequencies start from 0.12Hz. The controller will attempt to regulate the pressure fluctuations in the penstock, hence the regulation system will be unstable. k_p was decreased in Figure 7.2 to shift the crossover frequency away from the frequency of the pressure fluctuations, and thus obtaining a more stable system. However, this made the regulation system very slow with a crossover frequency of 0.045Hz.

8.5 Numerical results with air cushion surge chamber

The results from the simulation of Herand power plant without an air cushion surge chamber show that the regulation system was not stable. As previously mentioned, the simulations for Herand with an air cushion surge chamber was divided up into two phases; the complete system with a rigid penstock, and the penstock from the air cushion surge chamber to the turbine including the elastic property.

The Bode diagram for the rigid system shows (Figure 7.3):

The crossover frequency was 0.325Hz. The controller will attempt to regulate all fluctuations in pressure with frequencies below 0.325Hz. The crossover frequency can be moved to the right by increasing the gain k_p. This will make the system respond faster, but it also makes it less stable.

The frequency of the mass oscillations was 0.015Hz. These are slow oscillations in pressure that will be regulated by the controller. They will not cause instability in the control system because the mass oscillations are low-frequency fluctuations, and the frequency lie below the crossover frequency, by sufficient margin.

The Bode diagram for the elastic penstock from the air cushion surge chamber to the pipe shows (Figure 7.4):

The crossover frequency was 0.325Hz, which is the same as for Case 1. The frequency of the pressure fluctuations was above 2Hz. This is above the crossover frequency,

by sufficient margin, which means that the controller will not attempt to regulate these. The phase margin was 65 degrees, and $\Delta k = 9.8dB$. The requirements for stability is that phase margin should be 45 degrees or more and gain margin should be 6dB or more (Section 2.10). These requirements are fulfilled for Herand based on the simulations. Thus, Herand will obtain a stable regulation system when an air cushion surge chamber is implemented.

8.6 Other operating points

The system was analyzed with maximum turbine discharge as well, which is the dimensioning case. For that scenario, the downsurge of water in the air cushion surge chamber was $0.7575m$. The height of the water level inside the air cushion surge chamber is $2.31m$. Thus, there will not be downsurge of water into the pipe at operating point equal to maximum discharge for the turbine.

The numerical simulations with maximum discharge showed that the system was stable, and the crossover frequency was below the frequencies of the pressure fluctuations (Figure 7.5).

8.7 Comparison of numerical simulation and analytical approach

Without air cushion surge chamber

Both methods showed that the regulation system of Herand power plant will be unstable without an air cushion surge chamber (Figures 7.6 and 7.7). The crossover frequency was 0.35Hz, and the elastic frequency was 0.12Hz, for both methods. The analytical approach showed pressure fluctuations at higher frequencies than the numerical approach. The reason for this is unknown to the author, but it seems to be something within Simulink. One theory is that the Simulink method gets a problem when having to divide by zero, whereas the numerical approach avoids that.

With air cushion surge chamber

The two methods showed the same results for Herand power plant with an air cushion surge chamber, namely that the regulation system was stable (Figures 7.8 and 7.9). The same problem with the numerical simulation was displayed here too. However, both methods showed stability and they are consistent with each other apart from that. The crossover frequency was 0.325Hz, and the elastic frequency was above 2Hz for both methods. The phase margin for both methods was 65 degrees, and

$\Delta k = 9.8dB$. Thus, the stability analysis from both methods showed that Herand will obtain a stable regulation system.

9 Conclusion

The aim of this paper has been to examine whether Herand power plant can have a stable regulation system despite the fact that the topography at the location makes it challenging. In addition, the size of the plant puts it under the requirements to have frequency regulation and be able to operate in an isolated grid.

A stability analysis of Herand was conducted based on frequency response analysis. The numerical simulations from Simulink showed that the plant will obtain a stable regulation system with the presented controller parameters and the air cushion surge chamber dimensions and location. This was compared to an analytical approach conducted in Excel, which showed consistency with the numerical simulations. The volume of the air cushion was $527.6m^3$, the total volume of the air cushion surge chamber was $712.26m^3$, and it lies at a distance of 150m upstream the turbine. The results from the analytical calculations showed that potentially damaging downsurge of high-pressure air from the air cushion is avoided, and that the pressure change in front of the turbine is within acceptable limits.

In conclusion, based on the stability analysis conducted here, Herand power plant will obtain a stable regulation system when including an air cushion surge chamber.

10 Further work

Further work on Herand should include a detailed site analysis of the location. Whether the rock surrounding the air cushion surge chamber has acceptable quality and permeability should be investigated. This will give an indication of whether there is need for an implementation to prevent air leakage from the air cushion surge chamber. This will also give an indication of how much air refilling will be needed to keep the air pressure high in the air cushion. Measures to prevent leakage of air, as well as air refilling to the chamber, may become costly.

Further work should include verification of the methods used in this paper, which will minimize possible errors.

References

[1] H. Brekke, *Regulering av hydrauliske strømningsmaskiner.* Vannkraftlaboratoriet NTNU, 2003.

[2] A. Palmstrom, "Air cushion surge chamber - a cost-effective solution in hydropower design.," 2008.

[3] Sweco, "Konsesjonssøknad og konsesjonsutredning," 2010.

[4] J. Balchen, T. Andresen, and B. Foss, *Reguleringsteknikk.* Institutt for teknisk kybernetikk, NTNU, 5 ed., 2003.

[5] Statkraft, 2015.

[6] Statnett, "http://www.statnett.no/drift-og-marked/."

[7] Statnett, "Funksjonskrav i kraftsystemet (fiks)," 2012.

[8] T. K. Nielsen, "Cavitation and dynamic problems," *6th IAHR meeting of the Working Group*, 2015.

[9] T. K. Nielsen, "Dynamisk dimensjonering av vannkraftverk," report, SINTEF, 1990.

[10] R. Stople, *Dynamic Analysis of Hydropower plants.* Master's, 2012.

[11] T. K. Nielsen, "Air cushion," Konstruksjon, drift og vedlikehold av hydrauliske strømningsmaskiner.

[12] K. Rottmann, *Matematisk formelsamling.* Spektrum forlag, 2003.

[13] Sweco, *Kostnadsgrunnlag for vannkraftanlegg.* NVE, 2010.

A Full derivation of dynamic equations

A.1 Waterway

The equations relating volumetric flow, pressure and power are combined to find the correlation between power and guide vane position.

The equation of motion

$$g\frac{\partial H}{\partial x} + \frac{\partial v}{\partial t} + f\frac{v\,|v|}{2D} = 0 \tag{A.1}$$

Dividing by g and using the relation $v = \frac{Q}{A}$, give:

$$\frac{\Delta H}{L} + \frac{dQ}{dt}\frac{1}{gA} + f\frac{Q^2}{2gDA^2} = 0 \tag{A.2}$$

Multiplying the equation with L gives:

$$\frac{L}{gA}\frac{dQ}{dt} + \Delta H + KQ|Q| = 0 \tag{A.3}$$

Where $K = f\frac{L}{2gA^2D}$

Inserting the relation $h = \frac{\Delta H}{H_0}$, and assuming inelastic waterway for simplicity:

$$\frac{L}{gA}\frac{dQ}{dt} + hH_0 = 0 \tag{A.4}$$

and Laplace transforming gives the following equation.

$$\frac{L}{gA}\frac{1}{H_0}s\Delta Q + h = 0 \tag{A.5}$$

$$\frac{L}{gA}\frac{Q_0}{H_0}sq + h = 0 \tag{A.6}$$

Introducing $T_w = \frac{Q_0}{gH_0}\frac{L}{A}$

$$T_w sq + h = 0 \tag{A.7}$$

The equation for guide vane position is:

$$\kappa = \frac{Q}{Q_n}\frac{\sqrt{2gH_n}}{\sqrt{2gH}} \tag{A.8}$$

$$Q = \kappa\frac{Q_n}{\sqrt{H_n}}\sqrt{H} = \kappa k\sqrt{H} \tag{A.9}$$

Linearizing about the point (Q_0, H_0)

$$dQ = \kappa k\frac{1}{2}\frac{1}{\sqrt{H}}dH \tag{A.10}$$

$$\Delta Q = \kappa k\frac{1}{2}\frac{1}{\sqrt{H_0}}\Delta H \tag{A.11}$$

Multiplying with $(\sqrt{H_0})^2$

$$\Delta Q(\sqrt{H_0})^2 = \kappa k\frac{1}{2}\sqrt{H_0}\Delta H \tag{A.12}$$

Introducing $Q_0 = \kappa K\sqrt{H_0}$ gives

$$\Delta Q H_0 = \frac{1}{2}Q_0\Delta H \tag{A.13}$$

$$\frac{\Delta Q}{Q_0} = \frac{1}{2}\frac{\Delta H}{H_0} \tag{A.14}$$

Using the ratios $q = \frac{\Delta Q}{Q_0}$ and $h = \frac{\Delta H}{H_0}$ give

$$q = \frac{1}{2}h \tag{A.15}$$

The equation for power is:

$$P_h = \eta \rho g Q H \tag{A.16}$$

Linearizing and Laplace transforming give:

$$P_h = q + h \tag{A.17}$$

A.2 Surge shaft

The equation for changes in water level in the shaft is:

$$\frac{dz}{dt} = \frac{1}{A_s}(Q_{in} - Q_{out}) \tag{A.18}$$

Linearizing and Laplace transforming give:

$$szH_0 = \frac{1}{A_s}(q_{in} - q_{out})Q_0 \tag{A.19}$$

The final form of the shaft equation thus become:

$$z = \frac{1}{T_{up}}q_{sj} \tag{A.20}$$

Where $T_{up} = \frac{A_s H_0}{Q_0}$

A.3 Turbine Inertia

$$J\omega\frac{d\omega}{dt} = P_h - P_N = \Delta P \tag{A.21}$$

Laplace transforming gives

$$\omega_0 J \Delta\omega s = \Delta P \tag{A.22}$$

Multiplying with ω_0^2

$$J\frac{\Delta\omega}{\omega_0}s = \frac{\Delta P}{\omega^2}\frac{P_0}{P_0} \tag{A.23}$$

Using the relations $\nu = \frac{\Delta P}{P_0}$ and $\mu = \frac{\Delta n}{n_0}$ gives

$$\mu = \frac{1}{\frac{J\omega_0^2 s}{P_0}}\nu \tag{A.24}$$

Where $\frac{J\omega_0^2}{P_0} = T_a$= turbine inertia

$$\mu = \frac{1}{T_a s}\nu \tag{A.25}$$

A.4 Controller

The equation for a PID controller is:

$$\frac{dy}{dt} = -k_p\frac{dn}{dt} + \frac{k_p}{T_d}(n_0 - n) - k_p T_n \frac{d^2 n}{dt^2} \tag{A.26}$$

Laplace transforming gives

$$\Delta y s = -k_p \Delta n s + \frac{k_p}{T_d}\Delta n - k_p T_n \Delta n s^2 \tag{A.27}$$

Where $\Delta n = n_0 - n$ and $\Delta y = y_0 - y = -y$ because $y_0 = 0$

Multiplying A.27 with $\frac{n_0}{n_0}$ gives:

$$\Delta y s = k_p \Delta n \frac{n_0}{n_0}s + \frac{k_p}{T_d}\Delta n\frac{n_0}{n_0} + k_p T_n \Delta n \frac{n_0}{n_0}s^2 \tag{A.28}$$

Using the relation $\mu = \frac{\Delta n}{n_0}$ gives:

$$ys = k_p \mu n_0 s + \frac{k_p}{T_d} \nu n_0 + k_p T_n \mu s^2 \quad | \cdot \frac{1}{s\mu} \tag{A.29}$$

$$\frac{y}{\mu} = k_p n_o (1 + \frac{1}{T_d s} + T_n s) \tag{A.30}$$

$$\frac{y}{\mu} = \frac{1}{b_t} (1 + \frac{1}{T_d} + T_n s) \tag{A.31}$$

B Complete analytical calculations

Rated discharge

$$Q_r = \frac{19.75}{0.91 \cdot 1000 \cdot 9.81 \cdot (437 - 6.81)} = 5.14 m^3/s \tag{B.1}$$

Response time of the water masses

$$T_w = \frac{5.14}{9.81 \cdot 437}(\frac{800}{\pi} + \frac{1800}{2.0106}) = 1.38 s \tag{B.2}$$

And with air cushion surge chamber

$$T_w = \frac{5.14}{9.81 \cdot 437}\frac{150}{2.0106} = 0.089 s \tag{B.3}$$

Head loss

$$h_f = \frac{5.14^2}{2 \cdot 9.81}(\frac{0.015 \cdot 800}{\pi^2 \cdot 2} + \frac{0.016 \cdot 1800}{2.0106^2 \cdot 1.6}) = 6.81 mWC \tag{B.4}$$

Reflection time

$$T_R = \frac{2 \cdot 150}{1200} = 0.25 s \tag{B.5}$$

Pressure in front of the turbine without air cushion surge chamber

$$\Delta h = 2\frac{5.14 \cdot 2600}{10 \cdot 9.81 \cdot 2.0106} = 135.5 mWC \tag{B.6}$$

Pressure in front of the turbine with air cushion surge chamber

$$\Delta h = 2\frac{5.14 \cdot 150}{10 \cdot 9.81 \cdot 2.0106} = 7.8mWC \tag{B.7}$$

Thoma critical area

$$\alpha = \frac{fL}{2gD} = \frac{1}{2 \cdot 9.81}(\frac{0.015 \cdot 800}{2} + \frac{0.016 \cdot 1650}{1.6}) = 1.15 \tag{B.8}$$

$$A_{min} = 1.5\frac{1}{2 \cdot 9.81 \cdot 1.15 \cdot 437}((800 \cdot \pi) + (1650 \cdot 2.0106)) = 0.887m^2 \tag{B.9}$$

Volume of air cushion

$$V_0 = \frac{1.4 \cdot 420.2}{\frac{1}{0.887} - \frac{1}{80}} = 527.6m^3 \tag{B.10}$$

Amplitude of u-tube oscillations

$$\Delta h_{up} = 5.14\sqrt{\frac{800/\pi + 1650/2.0106}{9.81 \cdot 0.887}} + \frac{6.81}{3} = 59.4m \tag{B.11}$$

$$\Delta h_{down} = -5.14\sqrt{\frac{800/\pi + 1650/2.0106}{9.81 \cdot 0.887}} - \frac{6.81}{9} = -58m \tag{B.12}$$

Natural frequency of u-tube oscillations

$$\omega = \sqrt{\frac{9.81}{0.887(800/\pi + 1650/2.0106)}} = 0.1014rad/s \tag{B.13}$$

C Matlab code

Matlab code for values of variables in Simulink, elastic waterway

```
clc;
g = 9.81;
Q0 = 5.14;
H0 = 437;
a = 1200;

%Waterway
%Elastic, with air cushion surge chamber
L = 150;
A = 2.0106;
%Elastic, without air cushion surge chamber
%L = 2600;
%A = 2.0106;

hw = (Q0*a)/(2*A*g*H0);

%Turbine inertia
Ta = 6;

%PID controller
kp = 12;
Td = 3;
Tn = 0;
```

Matlab code for rigid system with air cushion surge chamber

```
clc;
g = 9.81;
Q0 = 5.14;
H0 = 437;
a = 1200;

% Turbine inertia
Ta = 6;

% Penstock before air cushion surge chamber
Lt2 = 2450;
At2 = 2.0106;
Tw = Q0/(g*H0)*(Lt2/At2);
Kt = 0.018;

% Penstock asfter air cushion surge chamber
Lt3 = 150;
At3 = 2.0106;
Tw2 = Q0/(g*H0)*(Lt3/At3);
Kt2 = 0.0011;
hw= (Q0*a)/(2*At3*g*H0);

% Air cushion surge chamber
Aeq = 0.887;
Tsj = Aeq*(H0/Q0);

kp = 12;
Td = 3;
Tn = 0;
```

D Some figures from the text in larger scale

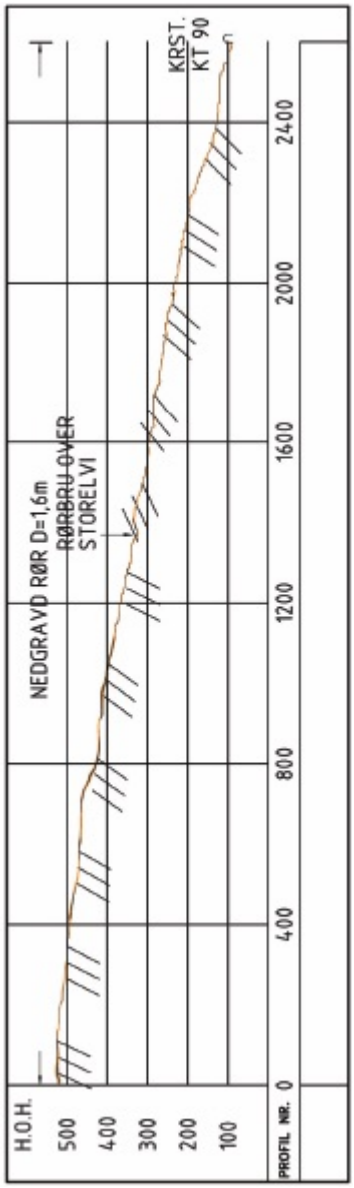

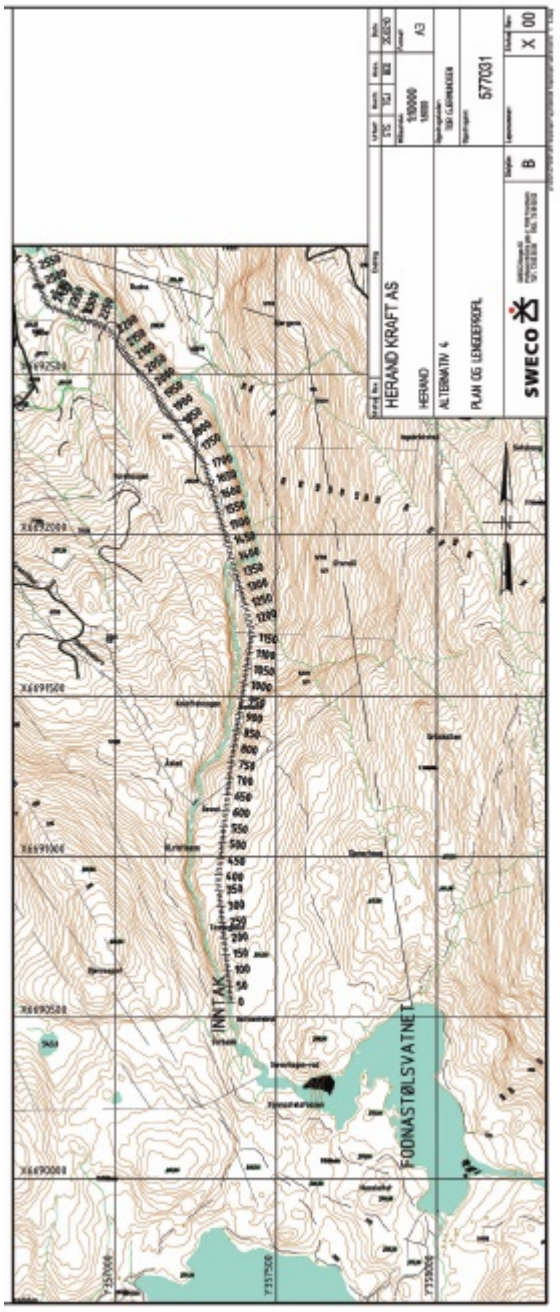

Figure D.2: Altitude profile no.2 [3]